



HAL
open science

Disruption of the blood-brain barrier and its close environment following adult exposure to low doses of di(2-ethylhexyl)phthalate alone or in an environmental phthalate mixture in male mice

Delnia Ahmadpour, Sakina Mhaouty-Kodja, Valérie Grange-Messent

► To cite this version:

Delnia Ahmadpour, Sakina Mhaouty-Kodja, Valérie Grange-Messent. Disruption of the blood-brain barrier and its close environment following adult exposure to low doses of di(2-ethylhexyl)phthalate alone or in an environmental phthalate mixture in male mice. *Chemosphere*, 2021, 282, pp.131013. 10.1016/j.chemosphere.2021.131013 . hal-03268559

HAL Id: hal-03268559

<https://hal.sorbonne-universite.fr/hal-03268559v1>

Submitted on 23 Jun 2021

HAL is a multi-disciplinary open access archive for the deposit and dissemination of scientific research documents, whether they are published or not. The documents may come from teaching and research institutions in France or abroad, or from public or private research centers.

L'archive ouverte pluridisciplinaire **HAL**, est destinée au dépôt et à la diffusion de documents scientifiques de niveau recherche, publiés ou non, émanant des établissements d'enseignement et de recherche français ou étrangers, des laboratoires publics ou privés.

1 **Title**

2 Disruption of the blood-brain barrier and its close environment following adult exposure to
3 low doses of di(2-ethylhexyl)phthalate alone or in an environmental phthalate mixture in male
4 mice

5 **Author names and affiliations:**

6 Delnia Ahmadpour, Sakina Mhaouty-Kodja and Valérie Grange-Messent*

7 Sorbonne Université, CNRS, INSERM, Neuroscience Paris-Seine, Institut de Biologie Paris-
8 Seine, 75005 Paris, France

9 ***Corresponding author**

10 Valérie Grange-Messent

11 Sorbonne Université, INSERM U1130, CNRS UMR 8246, Neuroscience Paris Seine, Institut
12 de Biologie Paris-Seine, 7 quai St Bernard, 75005, Paris, France.

13 Tel: +33 1 44 27 36 57

14 Fax: +33 1 44 27 25 08

15 e.mail: valerie.messent@sorbonne-universite.fr

16

17 **Abstract**

18 We have previously shown that adult male mice exposure to low doses of di(2-
19 ethylhexyl)phthalate (DEHP) alters neural function and behaviour. Whether such exposure
20 also affects the integrity and function of the blood-brain barrier (BBB) remained to be
21 explored. The impact of adult exposure to low doses of DEHP alone or in an environmental
22 phthalate mixture on the BBB integrity and surrounding parenchyma was studied in male

23 mice. Two-month-old C57BL/6J males were orally exposed for 6 weeks to DEHP alone (0.5,
24 and 50 µg/kg/day) or to DEHP (5 µg/kg/day) in an environmental phthalate mixture. BBB
25 permeability, glial activation and neuroinflammation were investigated in the hypothalamic
26 medial preoptic area (mPOA) and hippocampus involved, respectively on the reproductive
27 and cognitive functions. Exposure to DEHP alone or in a phthalate mixture increased BBB
28 permeability and affected the endothelial accessory tight junction protein zona occludens-1
29 and caveolae protein Cav-1 in the mPOA and the hippocampal CA1 and CA3 areas. This
30 was associated with an inflammatory profile including astrocyte activation accompanied by
31 enhanced expression of inducible nitric oxide synthase in the mPOA, and a microglial
32 activation in the mPOA and the hippocampal CA1 and CA3 areas. The protein levels of the
33 inflammatory molecule cyclooxygenase-2 were increased in activated microglial cells of the
34 exposed mPOA. None of the major effects induced by DEHP alone or in a mixture was
35 detected in the hippocampal dentate gyrus. The data highlight that environmental exposure
36 to endocrine disruptors such as phthalates, could represent a risk factor for the
37 cerebrovascular function.

38

39 **Keywords**

40 Blood–brain barrier, Endocrine disruptors, Phthalates

41

42 1. Introduction

43 Phthalates are chemical compounds found in plasticizers and solvents (Kabir et al., 2015)
44 and are among the most frequently detected organic pollutants in the environment. Di-2-
45 ethylhexyl phthalate (DEHP), the most commonly detected phthalate, is widely used to add
46 flexibility to high-molecular-weight polymers used in the manufacture of polyvinyl chloride
47 plastic and is therefore found in containers for the storage of food and beverages. DEHP was
48 also classified by the EU in 2000 as a priority substance “presenting a significant risk to or
49 via the aquatic environment” in the Water Framework Directive 2000/60/EC, which was
50 updated in 2008 and 2013 (Directive 2013/39/EU of the European Parliament and of the
51 Council of 12 August 2013). In addition to DEHP, other phthalates including diethyl phthalate
52 (DEP), dibutyl phthalate (DBP), butyl benzyl phthalate (BBP), and diisobutyl phthalate (DiBP)
53 are also detected in the environment worldwide (Gao and Wen, 2016).

54 The majority of the *in vivo* studies addressing the effects of phthalate exposure on the
55 nervous system have focused on the effects of perinatal exposure. Furthermore, the effects
56 of exposure to phthalates at low doses during adulthood are still largely under-explored. Our
57 recent study revealed that chronic exposure during adulthood to DEHP at the tolerable daily
58 intake dose (TDI) of 50 µg/kg/day (European Food Safety Authority (EFSA) 2005, 2019) or to
59 a 10-fold lower dose (5 µg/kg/day), close to environmental exposure, disrupts the emission of
60 courtship vocalizations and therefore the initiation of mating in male mice (Dombret et al.,
61 2017). This behavioural alteration was not due to modifications of circulating testosterone
62 levels and/or the integrity of the hypothalamic–pituitary–gonadal axis. It was instead
63 associated with down-regulation of the androgen receptor (AR) in the hypothalamic medial
64 preoptic area (mPOA), the main cerebral area involved in the expression of male sexual
65 behaviour (Dombret et al., 2017). The neural AR plays an important role in the expression of
66 male sexual behaviour (Raskin et al., 2009) and also in the modulation of hippocampal
67 functions as shown by the impaired temporal order memory in mice lacking the neural AR
68 (Picot et al., 2016). The male hippocampus does indeed exhibit high sensitivity to androgens

69 and can thus be targeted by compounds exhibiting anti-androgenic activities. In this context,
70 a previous study showed that prenatal or perinatal exposure to DEHP at 200 µg/kg/d or 10 to
71 200 mg/kg/d impaired spatial memory and induced anxiety- and depressive-like behaviour in
72 adult male mice, and that these effects were associated with AR down-regulation in the
73 hippocampus (Barakat et al., 2018; Xu et al., 2015).

74 In the brain, including the hypothalamus and hippocampus, the blood-brain barrier (BBB)
75 present at the level of the cerebral capillary protects cerebral regions from the toxicity of
76 circulating xenobiotics and pathogens thereby providing cerebral homeostasis (Weiss et al.,
77 2009). The BBB is formed by endothelial cells (ECs) which are themselves sealed by tight
78 junctions (TJs) and adherens junctions (Abbott et al., 2010; Weiss et al., 2009), thus limiting
79 the paracellular diffusion of substances. The BBB also provides a gate-like function for
80 substance delivery to brain cells by limiting trans-cellular diffusion via selective carrier-
81 mediated transport systems (Abbott et al., 2010). An extremely low rate of transendothelial
82 vesicular transport also integrates the transcellular pathway to minimize the uptake of
83 substances from blood to brain parenchyma (Villaseñor et al., 2019). Among the different
84 categories of vesicular transport, caveolae appears to be the major element responsible for
85 transcytosis in cerebral endothelial cells (Villaseñor et al., 2019). At their abluminal side, ECs
86 are surrounded by basal lamina embedding pericytes, and interact with glial cells (astrocytic
87 end-feet and microglial cells) and neurons. The whole is called the neurovascular unit (NVU)
88 (Erdő et al., 2017). The presence of glial cells in the vicinity of the BBB promotes NVU
89 susceptibility to neuroinflammatory responses. Neuroinflammation, in turn, can contribute to
90 BBB dysfunction and neurodegenerative process (Vodo et al., 2013).

91 Androgens were also shown to promote cerebral angiogenesis and vasculature formation,
92 and modulate the cerebrovascular function (see for review, Ahmadpour and Grange-
93 Messent, 2020). In particular, our previous data indicate that gonadal testosterone supports
94 the integrity and function of the BBB and prevents gliosis reaction and the up-regulation of
95 inflammatory proteins in adult male mice (Atallah et al., 2017) and rats (Barreto et al., 2007).

96 In this context, our work aims to document for the first time the impact of oral exposure
97 during adulthood to low doses of DEHP alone or in a phthalate mixture on the integrity of the
98 capillary BBB and surrounding parenchyma in male mice. Analyses were processed using
99 four experimental groups of adult C57BL/6J male mice exposed orally through contaminated
100 diet in order to mimic the major route of exposure as previously described (Adam et al.,
101 2021). The first three groups included males exposed for 6 weeks to the vehicle (control),
102 DEHP at the TDI dose of 50 µg/kg/d, or DEHP at 5 µg/kg/d. The DEHP dose of 5 µg/kg/d is
103 within the environmental exposure range; this dose induced behavioural alterations in male
104 mice following adult or pubertal exposure (Capela and Mhaouty-Kodja, 2021; Dombret et al.,
105 2017). In order to mimic environmental co-exposure to phthalates (Anses, 2015; Martine et
106 al., 2013), the fourth group of males was exposed for 6 weeks to a phthalate mixture
107 containing DEHP at 5 µg/kg/d, DBP at 0.5 µg/kg/d, BBP at 0.5 µg/kg/d, DiBP at 0.5 µg/kg/d
108 and DEP at 0.25 µg/kg/d. Analyses focused on two androgen-sensitive brain areas as
109 mentioned above the hypothalamic mPOA and the hippocampus. In these brain areas, we
110 investigated the effects of exposure on BBB permeability using exogenous tracer and
111 endogenous immunoglobulins G (IgG). Protein levels and distribution of TJ components as
112 well as glial activation and neuroinflammation were also assessed in the four exposed
113 groups.

114 **2. Material and Methods**

115 **2.1. Ethical statement**

116 The experiments have been reported in compliance with the Animal Research: Reporting in
117 Vivo Experiments (ARRIVE) guidelines. All studies were performed in compliance with the
118 National Institute of Health guidelines for the care and use of Laboratory Animals (NIH
119 Guide) and French and European legal requirements (Decree 2010/63/UE). Experiments
120 were performed accordingly, to minimize animal number and discomfort and were approved
121 by the “Charles Darwin” Ethical committee (project number 01490-01).

122 **2.2. Animals**

123 Males of C57BL/6j strain (Janvier Labs, Le Genest-Saint-Isle, France) bred in our laboratory
124 were housed in a conventional facility after weaning under controlled photoperiod (12:12h
125 light dark cycle-lights on at 1 p.m.), maintained at 22°C and relative humidity (60% ± 10%),
126 and had free access to water and a standard diet (A03–10; Safe-diets, Augy, France). The
127 mice were housed in nest-enriched polysulfone cages, with polysulfone bottles. Offspring
128 were mixed at the weaning to avoid potential litter effects with no more than one male per
129 litter per cage, and were allowed to grow to 8 weeks of age. For these experiments, 9 cohorts
130 each comprising 9 to 32 animals distributed equally between the 4 treatment groups, were
131 used. Ultimately, 32 animals from two cohorts were used for BBB permeability assays, 96
132 animals from five cohorts were used for the capillary-enriched fraction procedure and
133 Western blot analysis, and then 68 animals from three cohorts were used for the
134 immunocytochemistry study.

135

136 **2.3. Phthalate exposure**

137 Exposure to phthalates (Sigma Aldrich, Saint-Quentin Fallavier, France) was performed for 6
138 weeks as recently described (Adam et al., 2021). The phthalates were first dissolved in
139 absolute ethanol (1% of prepared food) and then in water (40% of prepared food) before
140 incorporated into food as previously described (Adam et al., 2021). Control animals were fed
141 with chow containing the vehicle i.e. ethanol and water (1% and 40% of prepared food,
142 respectively). Eight-week-old males were fed ad libitum with chow consisted of their normal
143 food containing the vehicle (control group), DEHP (CAS 117-81-7) at 50 or 5 µg/kg/d (DEHP-
144 50 and DEHP-5 groups, respectively), or a phthalate mixture (Mix group) containing DEHP at
145 5 µg/kg/d, DBP (CAS 84-74-2) at 0.5 µg/kg/d, BBP (CAS 85-68-7) at 0.5 µg/kg/d, DiBP (CAS
146 84-69-5) at 0.5 µg/kg/d and DEP (CAS 84-66-2) at 0.25 µg/kg/d, reconstituted into pellets as
147 precisely described previously (Adam et al., 2021). The composition of the phthalate mixture
148 was based on French and European studies showing an external co-exposure to these
149 molecules and the presence of their metabolites in urinary samples (Anses, 2015; Dewalque

150 et al., 2014; Martine et al., 2013). The ratio of DEHP to the other phthalates was determined
151 on the basis of the estimated daily intake in France and Europe (Dewalque et al., 2014;
152 Martine et al., 2013).

153 Mice were weighed weekly for the duration of the exposure and phthalate doses were
154 adjusted to their body weights and calculated for a daily food intake of 5 g per animal
155 (Dombret et al., 2017), on the basis of previous studies showing this average daily intake for
156 adult mice of 2 to 19 months old (Cheema et al., Br J Nutrition 2019). Body weight was
157 comparable between the four treatment groups on the first and last days of exposure
158 (supplementary Figure S1).

159 The analyses were performed on 5 cohorts each comprising animals distributed equally
160 between the 4 treatment groups. Briefly, two cohorts were used for BBB permeability assays,
161 two cohorts were used for immunohistochemistry study and then, one was used for the
162 capillary-enriched fraction procedure and Western blot analysis.

163 **2.4. BBB permeability assay**

164 The BBB permeability assay was performed using an exogenous tracer binding to serum
165 albumin, the Evans blue dye (Sigma Aldrich, Saint-Quentin Fallavier, France), and
166 endogenous IgG. The BBB restricts the passage of serum proteins such as albumin and
167 endogenous IgG from the blood flow into the interstitial tissue (Saunders et al., 2015).

168 **2.4.1. Evans Blue dye injection**

169 Three awake mice per treatment group were i.p. injected with a 2% Evans Blue solution (4
170 ml/kg) diluted in normal saline. Three hours later, the mice were deeply anaesthetized with a
171 lethal dose of pentobarbital (120 mg/kg, i.p.), then transcardially perfused with 0.9% saline
172 solution followed by 4% paraformaldehyde (PFA) solution diluted in 0.1M phosphate buffer
173 (PB) pH 7.4. Their brains were carefully removed and post-fixed with the same fixation
174 solution overnight at 4°C. Afterwards, the brains were cryoprotected with a 20% sucrose
175 solution for 24 hrs at 4°C before freezing in isopentane (-30°C) and 8 coronal sections (20

176 μm thick) included mPOA or hippocampus were cut using a cryostat and mounted on slides.
177 In order to visualize blood vessel walls, all sections were co-stained with anti-laminin rabbit
178 primary antibody (1/100; Table 1) followed by secondary Alexa488-conjugated anti-rabbit IgG
179 (1:1000, Invitrogen, Villebon sur Yvette, France). To avoid the Evans Blue dye spreading and
180 to promote optimal visualization of labelled fine structures, sections were quickly immersed in
181 xylene and mounted with a hydrophobic mounting medium using the method initially
182 developed by Werner et al., (Werner et al., 1997) and modified by (Atallah et al., 2017). The
183 Evans blue dye providing a red fluorescence (Steinwall and Klatzo, 1966), fluorescent
184 signals were observed under a confocal microscope (described below).

185 **2.4.2. Endogenous Immunoglobulin G detection**

186 Mice (n = 5 per treatment group) were deeply anaesthetized with a lethal dose of
187 pentobarbital (150 mg/kg, i.p.), then were transcardially perfused with 0.9% saline solution
188 followed by 4% PFA solution diluted in 0.1M PB pH7.4. Their brains were carefully removed
189 and post-fixed with the same fixation solution overnight at 4° C. Afterwards, the brains were
190 cryoprotected with a 20% sucrose solution for 24 hrs at 4°C before freezing in isopentane (-
191 30°C) and 8 coronal sections (20 μm thick) included mPOA or hippocampus were cut using a
192 cryostat and mounted on slides. The presence of extravasated endogenous mouse IgG from
193 blood to parenchyma was evaluated using Alexa488-conjugated anti-mouse IgG antibody
194 (1:1000, Invitrogen, Villebon sur Yvette, France) combined with immuno-labelling of laminin
195 as described above to detect microvessels. Then fluorescent staining was observed under a
196 confocal microscope (described below).

197 **2.5. Fluorescent immunohistochemistry**

198 The animals (n=5 per treatment group and per immuno-labelling) were deeply anaesthetized
199 with a lethal dose of pentobarbital (120 mg/kg, i.p.) for the following procedures.

200 **2.5.1. Tissue preparation**

201 The experiments were processed as previously described (Atallah et al., 2017). Briefly, for TJ
202 proteins (claudin-5, occludin and ZO-1) and the main component of caveolae plasma
203 membranes, Cav-1 protein, the brains were freshly removed and immediately frozen in
204 isopentane (-30°C). Six to eight serial frozen sections ($20\text{-}\mu\text{m}$ thickness) included mPOA
205 and hippocampus were cut and collected on slides, and were then fixed by immersion for 2
206 min at -20°C in methanol/acetone (vol/vol) with this followed by the labelling procedure. For
207 the other proteins (Iba-1, GFAP, S100 β , NDRG-2, Cox-2 and iNOS), male mice were deeply
208 anesthetized using i.p. injection of pentobarbital (120 mg/kg) diluted in with 0.9% saline
209 solution and then transcardially perfused with 0.9% saline solution followed by 4%
210 paraformaldehyde solution diluted in 0.1 M PB pH7.4. After post-fixation and cryoprotection
211 steps as described above, the brains were frozen in isopentane (-30°C) and 6 to 8 serial
212 frozen sections ($20\ \mu\text{m}$ thickness) included mPOA or hippocampus were cut using a cryostat
213 and collected on slides.

214 **2.5.2. Immuno-labelling procedure**

215 Non-specific sites were blocked by incubating slide-mounted sections in PBS 1X, 1% bovine
216 serum albumin (BSA) and 0.2% Triton X-100 for 1 h at room temperature. Then sections
217 were incubated with one or more primary antibodies (Table 1) overnight at 4°C diluted in the
218 same phosphate buffer saline (PBS)/bovine serum albumin (BSA)/Triton X-100 solution.
219 Immune complexes were revealed using secondary Alexa-conjugated anti-mouse, anti-goat
220 or anti-rabbit IgG (1:1000; Invitrogen, Villebon sur Yvette, France). Fluorescence was
221 observed with a confocal microscope.

222 **2.6. Confocal microscopy**

223 Simple and multiple fluorescent labelling was visualized with a SP5 upright Leica confocal
224 laser scanning microscope (Leica Microsystems) equipped with the Acousto-Optical Beam
225 Splitter (AOBS) and using 63x oil immersion objective. Alexa 488 was excited at 488nm and
226 observed from 495 to 580 nm; Alexa 555 was excited at 555 nm and observed from 599 to

227 680 nm. The gain and offset for each photomultiplier were adjusted to optimize detection
228 events. Images (1024x1024 pixels, 16 bits) were acquired sequentially between stacks to
229 eliminate cross-over fluorescence. The frequency was set up at 400 Hz and the pinhole was
230 set at 1 Airy. Each optical section (1 μm) was frame-averaged four times to enhance the
231 signal/noise ratio. Overlays, projection of the z-stack files and quantification were performed
232 using the Fiji software (NIH, USA). The presented pictures were the projection of 10–20
233 successive optical sections into one image, unless otherwise stated in the figure legend.
234 Quantification of the fluorescent density was performed on three sections sampled at the
235 level of the mPOA (plate 30 of the Mouse Brain Atlas of Paxinos and Franklin 2001) and on
236 three sections sampled at the level of the hippocampus (plate 48). The surfaces on which the
237 fluorescence density quantifications were performed are given in the figure legends.

238 **2.7. Western blot protein analysis using cerebral capillary-enriched factions**

239 ***2.7.1. Cerebral capillary-enriched fraction procedure***

240 Brains from 12 mice per treatment group were freshly removed and placed quickly on ice.
241 For each hypothalamic capillary-enriched fraction, two hypothalami were pooled (n = 6 per
242 treatment group), whereas one hippocampus was used for each hippocampal capillary-
243 enriched fraction (n = 6 per treatment group). Hypothalamic and hippocampal microvessels
244 were harvested according to a previously described method (Atallah et al., 2017; Sandoval
245 and Witt, 2011), in order to obtain microvessel-enriched fractions for each cerebral area.
246 Briefly, samples were homogenized in a pH 7.4 buffer containing 1% BSA, 2.7 mM KCl, 137
247 mM NaCl, 1.5 mM KH_2PO_4 , 8 mM Na_2HPO_4 , 1 mM CaCl_2 , 0.5 mM $\text{MgCl}_2 \cdot 6\text{H}_2\text{O}$, mM D-
248 glucose, 1 mM sodium pyruvate, 1 M 4-(2-Hydroxyethyl) piperazine-1-ethanesulfonic acid
249 (HEPES). Homogenates were centrifuged in an equal volume of 30% Ficoll for 15 min at
250 4800g at 4°C, supernatants were aspirated and pellets suspended in isolation buffer without
251 BSA and passed through a 70- μm nylon filter. Filtrates were centrifuged for 10 min at 4 °C at
252 3000g.

253 **2.7.2. Protein extraction**

254 Protein extraction from pellets of microvascular capillary fractions was performed with a RIPA
255 buffer containing 50mM Tris—base (pH 7.2), 10 mM EDTA, 10 mM EGTA, 150 mM NaCl,
256 0.1% sodium dodecyl sulfate, 0.5% deoxycholate acid, 1% Triton X-100, and 1% protease
257 inhibitor cocktail (Sigma Aldrich) and sonicated 10 times for 30 s. Homogenate samples were
258 centrifuged at 13000 rpm for 13 min at 4 °C and supernatants containing proteins were
259 collected. The total protein concentration of each sample was determined using the Bradford
260 Assay Kit (Thermo Scientific, Courtaboeuf-Villebon sur Yvette, France) according to the
261 manufacturer's protocol. Protein extracts were stored at -20°C until further processing.

262 **2.7.3. Electrophoresis and immunoblotting**

263 Protein samples were denatured in Laemmli Buffer and heated at 95°C for 5 min.
264 Electrophoretic migration of 10–20 µg of proteins was carried out on NuPAGE 4–12% Bis–
265 Tris Gel (Invitrogen, Villebon sur Yvette, France) or Mini-PROTEAN® TGX™ 7.5%
266 polyacrylamide gels (BIO-RAD, Marnes La Coquette, France). The resolved proteins were
267 then electrotransferred onto pre-treated polyvinylidene difluoride (PVDF) membranes
268 (Millipore, Molsheim, France).

269 Membranes with transferred proteins were blocked for 1 h, at RT with a solution of 5% non-
270 fat milk diluted in PBS 1X with 0.2 % Tween, and then incubated with primary antibodies
271 (Table 1) diluted in the same blocking solution overnight at 4 °C. Primary antibody binding to
272 blots was detected by incubation with respectively either secondary HRP–conjugated
273 (1:5000; Jackson, Cambridgeshire, United Kingdom) or biotin–conjugated (1:2000; Vector,
274 Burlingame, United States,) anti-rabbit, anti-mouse or anti goat for 2 h, at RT, and then
275 immune complexes were revealed by the SuperSignal™ West Pico or Femto
276 Chemiluminescent Substrate kit (Thermo Scientific, Courtaboeuf-Villebon sur Yvette,
277 France).

278 The signals were quantified by using Fiji software (NIH, USA) and normalized to the value
279 obtained for the corresponding housekeeper glyceraldehyde- 3-phosphate dehydrogenase
280 (GAPDH) protein band.

281 **2.8. Statistical analysis**

282 The four sample sizes corresponding to the vehicle-treated, DEHP-5 or DEHP-50 and
283 phthalate mixture were equal. Normal distribution of the four groups was checked using the
284 Shapiro-Wilk normality test then one-way ANOVA was used to analyze the main effects of
285 exposure and Tukey tests were used for posthoc analyses to determine group differences.
286 Differences were considered statistically significant if $p \leq 0.05$. In the text, means \pm S.E.M are
287 expressed as a percentage of the vehicle group. Two-way ANOVA was used to analyze the
288 effects of treatment on the body weight of exposed mice. Data are expressed as body weight
289 means (g) \pm S.E.M and differences were considered statistically significant if $p \leq 0.05$.

290

291 **3. Results**

292 **3.1. BBB permeability**

293 BBB permeability in the hypothalamic mPOA and hippocampal CA1, CA3 and DG sub-
294 regions was assessed in mice exposed to the vehicle or DEHP alone or in a phthalate
295 mixture by using exogenous Evans Blue dye (Figure 1; A-H), which binds to albumin protein,
296 and endogenous circulating IgG molecules (Figure 1; I-P). Detection of these tracers in the
297 parenchyma, called extravasation, indicates a BBB leakage. Therefore, to visualize blood
298 capillary walls, laminin, the main basal lamina protein, was immunodetected.

299 In the hypothalamic mPOA, fluorescent signal analyses showed treatment had had a
300 significant effect ($p \leq 0.01$) on the extravasation of the Evans Blue dye outside perfused brain
301 capillaries, with an increased extravasation in DEHP-5-, DEHP-50- and Mix-treated mice
302 (+110% $p \leq 0.01$, +130% $p \leq 0.01$ and +135% $p \leq 0.001$, respectively, above vehicle-treated
303 mice) determined by posthoc analyses (Figure 1A and B). In the hippocampus, the treatment

304 was found to have had an effect on the extravasation of the Evans Blue dye in the CA1 and
305 CA3 regions ($p \leq 0.0001$, $p \leq 0.01$, respectively). A significant increase above vehicle-treated
306 mice was evidenced by posthoc analyses for DEHP-5- and DEHP-50-treated mice in the
307 CA1 parenchyma (+95% $p \leq 0.01$ and +170% $p \leq 0.001$ respectively, $p \leq 0.05$), but only for
308 DEHP-50-treated mice in the CA3 parenchyma (+70%, $p \leq 0.05$) (Figure 1 C-F). In contrast,
309 there was no treatment effect in the DG capillaries, which greatly restricted Evans blue dye
310 extravasation to the brain parenchyma (Figure 1G and H).

311 Immunolabelling of endogenous circulating IgG showed that endogenous IgG were observed
312 and were restricted to capillary wall or lumen in vehicle-treated mice (Figure 1K and M). In
313 contrast, the effect of treatment on IgG immunoreactivity in the mPOA ($p \leq 0.01$), with higher
314 levels in DEHP-5, DEHP-50- and mixture-treated mice (+160%, $p \leq 0.01$; +35% and +15%, p
315 ≤ 0.05 ; respectively) in the parenchyma of phthalate-treated mice compared to the vehicle
316 group (Figure 1I and J) was shown by posthoc analyses. Similarly, a treatment effect ($p \leq$
317 0.0001) was found in the CA1 area with significantly higher levels of endogenous IgG in the
318 DEHP-5 (+140 %, $p < 0.05$), DEHP-50 (+270 %, $p < 0.01$) and Mix-groups (+900 %, $p <$
319 0.0001) versus the vehicle group (Figure 1K and L) was shown by posthoc analyses. There
320 was also a treatment effect in the CA3 area ($p \leq 0.0001$) as illustrated in Figure 1M and N;
321 posthoc analyses showed increased levels for mice exposed to DEHP alone or in a mixture
322 (+ 86%, +89% and +100%, $p \leq 0.0001$, for DEHP-5, DEHP-50 and mixture-group vs. vehicle,
323 respectively). In accordance with the result obtained for Evans blue dye, no extravasation of
324 circulating IgG from blood compartment to hippocampal DG parenchyma was detected
325 (Figure 1O and P).

326 **3.2. Protein levels and distribution of TJ components**

327 BBB leakage induced by DEHP alone or in a mixture could be due to an alteration of
328 capillary inter-endothelial TJs leading to paracellular transport of components. TJs comprise
329 a complex of transmembrane proteins claudin-5 and occludin, which are associated with
330 peripheral scaffolding proteins. Therefore, we investigated the distribution and amounts of

331 these proteins using immunofluorescence and Western blot analysis on microvessel-
332 enriched fractions. No significant effect of treatment was found on the protein amounts of
333 claudin-5 and occludin in the capillaries of hypothalamus (Figure 2A and B) and
334 hippocampus (Figure 2D and E). In addition, confocal microscopy analysis of the capillaries
335 of hypothalamic mPOA and hippocampal CA1, CA3 and DG sub-regions, showed no
336 significant treatment effect on the distribution of immuno-labelling of claudin-5
337 (supplementary figure S2) and occludin (supplementary Figure S3).

338 Those endothelial transmembrane components of TJs interact with the actin cytoskeleton via
339 cytoplasmic TJs accessory proteins with the ZO-1 protein having predominance. Data from
340 Western blot performed on microvessel-enriched fractions obtained from the hypothalamus
341 (Figure 2C), highlighted a treatment effect on ZO-1 protein amount ($p \leq 0.0001$), with less
342 ZO-1 for both DEHP-5- and DEHP-50-treated mice (-75%, $p \leq 0.0001$) and also Mix-treated
343 mice (-65%, $p \leq 0.0001$) versus the vehicle group following posthoc analyses. A treatment
344 effect was also found on the amount of ZO-1 in hippocampal capillaries (Figure 2F). Posthoc
345 analyses showed that the amount of ZO-1 was significantly increased for DEHP-50- treated
346 mice (+50%, $p \leq 0.05$), whereas no significant difference was detected for DEHP-5- and
347 mixture-treated groups compared to vehicle (Figure 2F). As for claudin-5 and occludin,
348 confocal microscopy analysis of the capillaries of hypothalamic mPOA and hippocampal
349 CA1, CA3 and DG sub-regions, showed no treatment effect on the immuno-labelling of ZO-1
350 protein (supplementary Figure S4).

351 **3.3. Cav-1 protein level in capillaries walls**

352 Caveolae are non-clathrin-coated vesicles with plasma membranes enriched in caveolin
353 (Cav) proteins, involved in the receptor-independent transcellular transport of molecules from
354 blood to parenchyma. We analyzed the level of caveolin-1 isoform protein (Cav-1), the main
355 component of the caveolae plasma membranes. Fluorescence analysis revealed an effect of
356 treatment ($p \leq 0.01$) on Cav-1 immunoreactivity in capillary walls and posthoc analyses
357 showed a significant high decrease for DEHP-50- and Mix-treated mice in the mPOA (DEHP-

358 50 group: -50 %; $p < 0.05$ and mixture-group: -75%; $p < 0.01$ vs. vehicle; Figure 3A and B)
359 and in the CA-1 (DEHP-50 group: -60 %; $p < 0.05$ and mixture-group: -70%; $p < 0.01$ vs.
360 vehicle; Figure 3D and E) and CA-3 areas (-70 %; $p < 0.01$ vs. vehicle in DEHP-50 and
361 mixture-group; Figure 3F and G). Again, no significant treatment effect was found in
362 hippocampal DG (Figure 3H and I). These results were confirmed by Western blot analysis
363 performed on microvessel-enriched fractions showing a treatment effect ($p \leq 0.001$), with a
364 decrease by -63% and -56% ($p < 0.01$ in DEHP-50 and mixture-group, respectively) in
365 hypothalamic vessels (Figure 3C) and -60% ($p < 0.01$) and -50% ($p < 0.05$) in hippocampal
366 vessels of DEHP-50 and mixture-group respectively in comparison to the vehicle group
367 (Figure 3J) determined by posthoc analyses.

368 **3.4. Glial activation and neuroinflammation**

369 The neuroinflammation process occurs following several brain insults and is often associated
370 with a dysfunction of the neurovascular unit. Neuroinflammatory responses are underlined on
371 the one hand by a glial activation involving an increase of glial specific protein levels,
372 NDRG2, S100 β and GFAP for astrocyte, and Iba-1 for microglia, and on the other hand by
373 an increase of inflammatory molecules such as iNOS and COX-2. The distribution of these
374 proteins was assessed using immunofluorescence, and protein levels in glial cells closely
375 associated with capillaries were assessed using Western blot analysis performed on
376 microvessel-enriched fractions from the whole hypothalamus and hippocampus.

377 In the mPOA, analyses of immunofluorescence results showed an effect of treatment on
378 NDRG2 and S100 β labellings ($p \leq 0.0001$; $p \leq 0.05$, respectively). A significant increase of
379 NDRG2 labelling in astrocytes for mixture-treated mice (+125%, $p < 0.0001$ vs. vehicle,
380 Figure 4A and B) and a significant increase of S100 β labelling in astrocytes for DEHP-50-
381 and mixture-treated mice (+92% and +82% vs. vehicle, respectively, $p < 0.05$, Figure 4A and
382 C) were determined by posthoc analyses. All NDRG2-positive astrocytes are immunoreactive
383 for S100 β but few S100 β -positive astrocytes express NDRG2. This astrocytic activation was
384 confirmed by a significant enhancement of GFAP immunofluorescence density in the

385 parenchyma and in the vicinity of capillaries for DEHP-50-treated mice (+ 100%; $p < 0.05$ vs.
386 vehicle, Figure 4D and E). By contrast, Western blot analysis performed on microvessel-
387 enriched fractions showed an effect of treatment ($p \leq 0.0001$), with a significant decrease of
388 GFAP amount in the astrocytic end-feet which remained in contact with the isolated vessels
389 for DEHP-5-, DEHP-50- and mixture-treated mice compared to vehicle (-40%, $p < 0.01$, -
390 55%, $p < 0.0001$ and -37%, $p < 0.01$, respectively vs. vehicle, Figure 4G), determined by
391 posthoc analyses.

392 Immunofluorescent analysis showed an effect of treatment ($p \leq 0.01$), with a stronger signal
393 for iNOS colocalized with GFAP surrounding capillaries not only for DEHP-5-, DEHP-50-
394 treated mice (+280 %; $p < 0.01$ vs. vehicle) but also for mixture-treated mice compared to
395 vehicle (+360 %; $p < 0.001$ vs. vehicle) (Figure 4D and F). Conversely, no significant effect
396 was highlighted for iNOS protein level using Western blot analysis performed on
397 hypothalamic microvessel-enriched fractions (Figure 4H). Immunohistochemical labelling for
398 the specific marker of microglial cells, Iba-1, was also changed by the treatment ($p \leq 0.01$)
399 and posthoc analyses showed a significant increase in the mPOA parenchyma for DEHP-50-
400 treated mice (+125%; $p < 0.01$ vs. vehicle, Figure 6A and B), whereas hypothalamus
401 capillary-enriched fraction showed no difference in the amount of Iba-1 protein among the
402 experimental groups (Figure 6C). COX-2 protein was immuno-detected in Iba-1-
403 immunopositive microglial cells in the mPOA (Figure 6A) especially for DEHP-50-treated
404 group compared to vehicle (+130 %; $p < 0.01$, Figure 6D). However, no significant difference
405 in the COX-2 protein amount was measured in the capillaries of hypothalamus of phthalate-
406 treated mice compared to those of vehicle-treated mice (Figure 6E).

407 In the hippocampus, analysis of the environment of the capillaries of CA1, CA3 and DG sub-
408 regions showed no significant treatment effect for immuno-labelling intensity of NDRG2 and
409 S100 β for all phthalate-treated groups compared to the vehicle (Figure 5A-F). Observations
410 using confocal microscopy confirmed these results (supplementary figure S5). Quantification
411 of GFAP immunoreactivity displayed no significant treatment effect between control and

412 phthalate-treated mice not only in the CA1 (Figure 5G and H) but also in the CA3 (Figure 5J
413 and K) and in the DG region (Figure 5M and N). Western blot analysis performed on
414 hippocampal microvessel-enriched fractions did not show any modification of GFAP protein
415 content in the hippocampus, regardless of the experimental group (Figure 5P).
416 Immunofluorescent analysis showed that iNOS labelling was not co-localized with GFAP
417 labelling in the CA1 region (Figure 5G), but was significantly impacted by the treatment ($p \leq$
418 0.01) and enhanced for DEHP-5-, DEHP-50 and mixture-treated mice compared to the
419 vehicle (+180 %; $p < 0.01$, +125 %; $p < 0.05$, and +115 %; $p < 0.05$, respectively vs. vehicle,
420 Figure 5I) determined by posthoc analyses. In the hippocampal CA3 region, the level of
421 iNOS immunoreactivity, not detected in astrocyte (Figure 5J), was equivalent between
422 animals treated with the vehicle and DEHP alone or in a mixture (Figure 5L). In the
423 hippocampal DG, iNOS immunoreactivity was affected by the treatment ($p \leq 0.001$) and
424 significantly increased only for DEHP-5-treated mice (+270%; $p < 0.001$, vs. vehicle, Figure
425 5O). Finally, no effect on iNOS protein amount was measured (Figure 5Q) in the
426 hippocampal microvessels.

427 Iba-1 immunoreactivity was affected by treatment ($p \leq 0.05$) and increased in the CA1
428 (+115%, + 125% and + 118%; $p < 0.05$ vs. vehicle in DEHP-5, DEHP-50 and mixture-group
429 respectively; Figure 6F and G), and in CA3 areas (DEHP-5 group: + 200%; $p < 0.0001$;
430 DEHP-50 group: + 90 %; $p < 0.05$; mixture-group: + 80%; $p < 0.05$ vs. vehicle; Figure 6I and
431 J). No treatment effect was measured in the DG (Figure L and M). In the hippocampal
432 capillaries-enriched fractions, no significant treatment effect was observed on the protein
433 amounts of Iba-1 (Figure 6O). Confocal microscopy and Western blot analysis showed no
434 significant effect on COX-2 immunolabelling (Figure 6H, K and N) and the amount of protein
435 in microvessel-enriched fractions of the hippocampus (Figure 6P).

436 **4. Discussion**

437 This study aimed to characterize the impact of a subchronic oral exposure to environmental
438 doses of DEHP alone or in a phthalate mixture on the neurovascular unit in the
439 hypothalamus and hippocampus of adult male mice. To our knowledge of the available
440 literature, this study is the first to assess the effects of adult exposure to low doses of
441 phthalates on the blood-brain barrier.

442 The data obtained show that exposure to DEHP alone or in a phthalate mixture significantly
443 increased the BBB permeability in the hypothalamic mPOA and the hippocampal CA1 and
444 CA3 regions as evidenced by the use of two different techniques assessing extravasation of
445 exogenous Evans blue tracer and circulating endogenous IgG. It is generally accepted that
446 increased permeability of the BBB reflects the failure of its functional integrity (Erdő et al.,
447 2017), which can be manifested by an alteration at the molecular and / or morphological level
448 of the constituents of these TJs (Obermeier et al., 2013). Our results show that exposure to
449 DEHP alone or in a phthalate mixture did not affect the expression of the major TJs
450 transmembrane proteins, claudin-5 and occludin, indicating that the increased BBB
451 permissiveness was not due to changes in these protein amounts in the two brain structures
452 we assessed. Our results show that the increased BBB permeability induced by exposure to
453 DEHP alone at 5 or 50 µg/kg/d or DEHP 5 µg/kg/d in a phthalate mixture was associated with
454 a dramatically decreased amount of the accessory junctional protein ZO-1 in hypothalamic
455 microvessel-enriched fractions. An opposite effect was observed in hippocampal
456 microvessel-enriched fractions in the group exposed to DEHP at 50 µg/kg/d. The underlying
457 cause of these changes could, at least in part, be the observed BBB integrity failure induced
458 by exposure to DEHP alone or in a mixture, since interaction between claudin, occludin and
459 ZO-1 is pivotal for facilitating tight junction assembly, and regulating the effectiveness of TJs
460 complex function (Abbott et al., 2010). However, it is important to note that no difference was
461 detected in ZO-1 immunoreactivity when assessed by immunohistochemistry in the mPOA,
462 or CA1 and CA3 regions. A possible explanation could be that in the brain sections submitted
463 to immunohistochemical analyses, the quantifications were carried out from 2-dimensional

464 images and therefore the absence of the third dimension may impede the complete
465 evaluation of the components of TJ proteins.

466 In addition to this possible impairment in the organization of endothelial TJs, our results also
467 highlight potential modifications in caveolae-mediated transcellular transport. Indeed, adult
468 exposure to DEHP at 50 µg/kg /d or to DEHP 5 µg/kg /d in the phthalate mixture led to a
469 significant decrease in Cav-1 immunoreactivity in the mPOA and CA1 and CA3 regions, and
470 in the amount of protein of the microvessel-enriched fractions of the hypothalamus and
471 hippocampus.

472 In the DG, none of the modifications induced by phthalate exposure on BBB permeability and
473 amounts of proteins involved in endothelial TJs and Cav-1 were observed, indicating that
474 BBB integrity was preserved in this hippocampal vascular network. These results suggest
475 that, within the same brain structure, the BBB may exhibit differential sensitivity to exposure
476 to DEHP alone or in a mixture. This difference in sensitivity within the hippocampus suggests
477 that maintaining BBB would involve different signalling pathways, with the DG containing
478 neural circuits different from those of the CA1 and CA3 subregions and being the site of adult
479 neurogenesis.

480 The modifications induced by exposure to DEHP alone or in a phthalate mixture in the BBB
481 integrity were associated with astrocyte and microglial activation in the hypothalamic mPOA.
482 Astrocyte activation was characterized by the increased immunoreactivity for both GFAP,
483 NDRG2 and S100β in the parenchyma of the mPOA. Firstly, this is in accordance with our
484 recent study reporting that chronic adult exposure to DEHP at 50 µg/kg/d induced an up-
485 regulation of GFAP in the parenchyma of the mPOA in male mice (Dombret et al., 2017).
486 Secondly, the data also indicate that adult exposure of male mice to DEHP alone or in a
487 phthalate mixture was capable of affecting different steps of cellular activation and states.
488 NDRG2 is induced in the early phase of astrocyte activation preceding GFAP expression (Lin
489 et al., 2015), while S100β is defined as a state in which astrocytes lose their neural stem cell
490 potential and acquire a more mature developmental stage (Raponi et al., 2007). Western blot

491 analysis performed with hypothalamic microvessel-enriched fractions showed a decreased
492 GFAP amount in astrocyte end-feet associated with microvessels. This difference in the data
493 protein obtained between the two techniques suggests a reorganization of the intermediate
494 filament cytoskeleton of astrocytes involved in the BBB. Reactive astrocytes are known to
495 express the pro-inflammatory molecule iNOS in response to various stimuli to produce an
496 excessive amount of nitric oxide (NO), a gaseous signalling molecule involved in most cases
497 with a neurodegenerative and neuroinflammatory status (Saha and Pahan, 2006). A Western
498 blot performed on microvessel-enriched fractions from the whole hypothalamus showed no
499 changes in the iNOS protein levels, but higher iNOS labelling was colocalized with GFAP
500 labelling astrocyte end-feet associated with capillaries in the mPOA. This suggests that the
501 inflammatory reaction mediated by astrocytes was initiated at, or limited to, the level of the
502 BBB. The astroglial activation in the parenchyma of the mPOA induced by the exposure to
503 DEHP at 50 µg/kg/d was accompanied by an activation of microglial cells, which also
504 exhibited a higher immunoreactivity of the inflammatory molecule COX-2. The association
505 between COX-2 expression and microglial activation could lead to NVU impairment through
506 neuronal damage as has been previously reported (Vijitruth et al., 2006). Further studies will
507 compare the impact of phthalate exposure on neuronal integrity.

508 In the hippocampus, no changes in astrocyte activation markers were induced by adult
509 exposure to DEHP alone or in a phthalate mixture, suggesting an absence of astrocyte
510 activation in this region despite the increased BBB permeability. In contrast, microglial
511 activation was observed in the CA1 and CA3 sub-regions following exposure to DEHP alone
512 or in a phthalate mixture, whereas no changes in COX-2 immunoreactivity were
513 demonstrated. A recent investigation has shown that prenatal exposure to DEHP at 200
514 µg/kg/d increased the level of COX-2 in pyramidal neurons of the CA-2/3 region in adult male
515 mice (Barakat et al., 2018). This suggests that differences in induced COX-2 expression by
516 phthalates may depend on the period of exposure. Alternatively, a longer exposure period in
517 adult males may be a more efficient way of inducing astrocyte activation and COX2

518 expression. Nevertheless, exposure to DEHP alone or in a mixture-induced iNOS activation
519 was noted in the CA1 and DG sub-regions but not in the CA3 area, while BBB leakage was
520 detected in both the CA1 and CA3 areas. The iNOS labelling was thus not colocalized with
521 the astrocytic marker GFAP, suggesting that astrocytes of the BBB may not be the only cells
522 capable of producing NO under these conditions. Indeed, different brain cell types including
523 neurons, macrophages and microglia, can respond to different stimuli with iNOS production
524 and take part in brain inflammation (Heneka and Feinstein, 2001; Sierra et al., 2014). It is
525 thus possible that an increased amount of iNOS protein in the hippocampus may arise from
526 an additional direct impact of DEHP alone or in a mixture on the parenchyma. Phthalates are
527 able to cross the BBB thus eliciting direct effects through neuronal damage,
528 neuroinflammation, oxidative stress and alteration of monoaminergic, cholinergic and amino-
529 acids transmission as has been reported for adult or developmental exposure to DEHP or
530 DBP at high doses ranging from 30 to 750 mg/kg/d (Kassab et al., 2019; You et al., 2018).
531 Thus, the question remains as to whether the BBB dysfunction is a cause or a consequence
532 of a neuroinflammatory state.

533 Altogether, these data show that the BBB dysfunction and generally associated astroglial
534 activation and neuroinflammation were differently induced by adult exposure to DEHP alone
535 or in a phthalate mixture (Table 2). Differences were seen between the hypothalamic mPOA
536 and hippocampus, in particular for the astrocyte activation. Differences in sensitivity to
537 exposure were also suggested by the obtained data for each brain area. In the mPOA, while
538 BBB permeability and iNOS induction were affected since 5 µg/kg/d of DEHP alone or in a
539 mixture, the other parameters were rather altered at 50 µg/kg/d of DEHP and /or the mixture,
540 suggesting that the other phthalates add to the effects of DEHP-5. In the hippocampus, the
541 DG appeared less sensitive showing only an induced iNOS in response to DEHP treatment
542 while the CA1 and CA3 areas were more reactive, with effects induced since 5 µg/kg/d of
543 DEHP alone for BBB permeability, microglial activation and neuroinflammation.

544 The down-regulation of the androgen receptor (AR) induced by exposure to DEHP in the
545 hypothalamic mPOA has been previously shown (Dombret et al., 2017). Thus, the alterations
546 triggered by adult exposure to DEHP alone or in a phthalate mixture in the neurovascular unit
547 of the mPOA may be also linked, at least in part, to the down-regulation of the AR.
548 Furthermore, in another study, we have shown that testosterone depletion in adult male
549 mice, leading to a down-regulation of the neural AR, triggered i) BBB permeability for Evans
550 Blue and endogenous IgG with a disorganization of TJ structure including a reduced protein
551 amount of ZO-1, ii) increased activation of astrocytes and microglia and iii) up-regulation of
552 inflammatory molecules such as iNOs and COX2 (Atallah et al., 2017). Finally, the AR
553 mediated-transcriptional activity is, at least in part, positively modulated by the caveolae
554 transmembrane Cav-1 protein (Bennett et al., 2010; Lu et al., 2001). The tight regulation by
555 androgens of several proteins involved in these processes is detailed in a recent review
556 (Ahmadpour and Grange-Messent, 2020).

557 The hippocampus is also an androgen-sensitive area, as evidenced by a high AR expression
558 in male mice and altered related functions in a mouse model lacking the neural AR
559 (Mhaouty-Kodja, 2018; Picot et al., 2016; Raskin et al., 2009). It is thus possible that the
560 alterations reported here in the neurovascular unit of this structure may also depend, at least
561 in part, on an impact on the AR signalling pathway. This can explain the comparable data
562 obtained on BBB permeability, endothelial TJs and trans-endothelial vesicular transport in
563 the mPOA and CA1 and CA3 regions following exposure to DEHP alone or in a phthalate
564 mixture (Table 2). The CA1 and CA3 regions contain much more AR-immunoreactive
565 neurons than the DG (Raskin et al., 2009), which may explain the reduced sensitivity of this
566 latter area to DEHP exposure.

567 The differences observed in astrocyte activation and COX-2 expression between the mPOA
568 and the hippocampal CA1 and CA3 regions, and also within the same brain area for the
569 different components of the neurovascular unit could be underlined by different expression
570 patterns of AR but also of estrogen receptors (ERs) in neurons, endothelial cells, astrocytes

571 and microglia, which also express these receptors (Hajszan et al., 2007; Kerr et al., 1995;
572 Picot et al., 2016). Indeed, in the male rodent nervous system, testosterone exerts its effects
573 through direct activation of the AR, but can also be metabolized into estradiol, which then
574 stimulates ER α and ER β .

575 The effects induced by DEHP exposure i.e. BBB permeability, astroglial activation and
576 neuroinflammation in adult male mice may participate, in particular in the mPOA, to the
577 altered sexual behaviour observed under similar experimental conditions (Dombret et al.,
578 2017). Current studies explore the cognitive impact of male mice exposure to low doses of
579 phthalate but only one recent study addressed the effects of adult DEHP exposure on spatial
580 learning and memory at high doses of 100 and 300 mg/kg/d in male rats (Ran et al., 2019).
581 Besides behavioural alterations, the BBB leakage and inflammatory signs induced by oral
582 exposure to low doses of phthalates reported in the present study may participate in other
583 neural alterations. Although they appear moderate, these modifications could have
584 deleterious long-term consequences in the case of chronic environmental exposure. Indeed,
585 BBB impairment and neuroinflammation are suspected to be involved in neurodegenerative
586 diseases and aging processes (Erdő et al., 2017).

587 Our analyses addressing the impact of DEHP exposure on behavioural responses (Dombret
588 et al., 2017) and BBB integrity (present study) in male mice show that DEHP-induced effects
589 can be observed at low doses equivalent or below the tolerable daily intake dose of 50
590 $\mu\text{g}/\text{kg}/\text{d}$, which was established and recently updated by the European Food Safety Authority
591 on the basis of reduced fetal testosterone production. This indicates that the nervous system
592 including the neurovascular unit is highly sensitive to phthalates and should be also
593 considered as a relevant endpoint in risk assessment for these molecules. In this context, it
594 is important to stress that the human cerebrovascular function also seems sensitive to
595 androgen, although these effects are less defined than for estrogens (see for review,
596 (Robison et al., 2019)).

597 **5. Conclusion**

598 The present study shows that phthalates, a family of endocrine disruptors, can impact the
599 cerebrovascular function at doses close to the environmental exposure in adult male mice.
600 Subchronic exposure to low doses of DEHP alone or in a phthalate mixture increases BBB
601 permeability of two brain regions leading to a dysfunctionality of this selective interface,
602 which is needed to ensure a tight regulation between the circulatory system, the immune
603 system and the brain parenchyma. In addition, we also show similarities and differences in
604 the vulnerability of the NVU of the two brain regions, one controlling male sexual behaviour,
605 and the second one involved in cognitive function. Based on our previous studies, we
606 suggest that phthalates may operate through a mode of action involving at least a partial
607 disruption of neural *AR* expression in the mPOA, but the ER and/or other signalling pathways
608 may be also involved in the hippocampus.

609 These data suggest that exposure to endocrine disruptors may be considered as an
610 environmental risk factor for the cerebrovascular function.

611

612 **Author contributions**

613 **Delnia Ahmadpour:** Investigation, Formal analysis, Writing-original draft. **Valérie Grange-**
614 **Messent:** Conceptualization, Supervision, Writing-review & editing. **Sakina Mhaouty-Kodja:**
615 Funding acquisition, Review & editing.

616

617 **Declaration of Interest Statement**

618 The authors declare they have no actual or potential competing financial interests or
619 personal relationships that could have appeared to influence the work reported in this paper.

620

621 **Acknowledgments**

622 This work was supported by the Agence Nationale de la Recherche (Phtailure, 2018). We
623 thank the rodent facility of the Institut de Biologie Paris-Seine (IBPS, Paris, France) for taking
624 care of the animals and the IBPS Imaging facility (confocal microscopy).

625

626 **References**

627 Abbott, N.J., Patabendige, A.A.K., Dolman, D.E.M., Yusof, S.R., Begley, D.J., 2010.
628 Structure and function of the blood-brain barrier. *Neurobiol. Dis.* 37, 13–25.
629 <https://doi.org/10.1016/j.nbd.2009.07.030>

630 Adam, N, Brusamonti, L, Mhaouty-Kodja, S., 2021. Exposure of adult female mice to low
631 doses of di(2 ethylhexyl)phthalate alone or in an environmental phthalate mixture: Evaluation
632 of reproductive behavior and underlying neural mechanisms. *Environ Health Perspect*, 129
633 (1). <https://doi.org/10.1289/EHP7662>

634 Ahmadpour, D., Grange-Messent, V., 2020. Involvement of testosterone signaling in the
635 integrity of the neurovascular unit in the male: review of evidence, contradictions and
636 hypothesis. *Neuroendocrinology*. <https://doi.org/10.1159/000509218>

637 Anses. 2015. Connaissances relatives à la réglementation, à l'identification, aux propriétés
638 chimiques, à la production et aux usages des composés de la famille des Phtalates (Tome3).
639 <https://www.anses.fr/fr/system/files/SUBCHIM2009sa0331Ra-106.pdf>

640 Atallah, A., Mhaouty-Kodja, S., Grange-Messent, V., 2017. Chronic depletion of gonadal
641 testosterone leads to blood–brain barrier dysfunction and inflammation in male mice. *J.*
642 *Cereb. Blood Flow Metab.* 37, 3161–3175. <https://doi.org/10.1177/0271678X16683961>

643 Barakat, R., Lin, P.-C., Park, C.J., Best-Popescu, C., Bakry, H.H., Abosalem, M.E.,
644 Abdelaleem, N.M., Flaws, J.A., Ko, C., 2018. Prenatal Exposure to DEHP Induces Neuronal
645 Degeneration and Neurobehavioral Abnormalities in Adult Male Mice. *Toxicol. Sci. Off. J.*
646 *Soc. Toxicol.* 164, 439–452. <https://doi.org/10.1093/toxsci/kfy103>

647 Barreto, G., Veiga, S., Azcoitia, I., Garcia-Segura, L.M., Garcia-Ovejero, D., 2007.
648 Testosterone decreases reactive astroglia and reactive microglia after brain injury in male
649 rats: role of its metabolites, oestradiol and dihydrotestosterone: Testosterone down regulates
650 reactive gliosis. *Eur. J. Neurosci.* 25, 3039–3046. [https://doi.org/10.1111/j.1460-](https://doi.org/10.1111/j.1460-9568.2007.05563.x)
651 [9568.2007.05563.x](https://doi.org/10.1111/j.1460-9568.2007.05563.x)

652 Bennett, N.C., Gardiner, R.A., Hooper, J.D., Johnson, D.W., Gobe, G.C., 2010. Molecular
653 cell biology of androgen receptor signalling. *Int. J. Biochem. Cell Biol.* 42, 813–827.
654 <https://doi.org/10.1016/j.biocel.2009.11.013>

655 Capela, D., Mhaouty-Kodja, S., 2021. Effects of pubertal exposure to low doses of di-(2-
656 ethylexyl)phthalate on reproductive behaviors in male mice. *Chemosphere* 263, 128191.
657 <https://doi.org/10.1016/j.chemosphere.2020.128191>

658 Cheema, U.B., Most, E., Eder, K., Ringseis, R., 2019. Effect of lifelong carnitine
659 supplementation on plasma and tissue carnitine status, hepatic lipid metabolism and stress
660 signalling pathways and skeletal muscle transcriptome in mice at advanced age. *Br. J.*
661 *Nutrition* 121 (12), 1323-1333. <https://doi.org/10.1017/S0007114519000709>

662 Directive 2013/39/EU of the European Parliament and of the Council amending Directives
663 428 2000/60/EC and 2008/105/EC as regards priority substances in the field of water policy.
664 Available 429 at: [https://www.ecolex.org/details/legislation/directive-201339eu-of-the-](https://www.ecolex.org/details/legislation/directive-201339eu-of-the-european-parliament-and430-of-the-council-amending-directives-200060ec-and-2008105ec-as-regards-priority-substances-in-the431-field-of-water-policy-lex-faoc127344/)
665 [european-parliament-and430](https://www.ecolex.org/details/legislation/directive-201339eu-of-the-european-parliament-and430-of-the-council-amending-directives-200060ec-and-2008105ec-as-regards-priority-substances-in-the431-field-of-water-policy-lex-faoc127344/)
666 [of-the-council-amending-directives-200060ec-and-2008105ec-](https://www.ecolex.org/details/legislation/directive-201339eu-of-the-european-parliament-and430-of-the-council-amending-directives-200060ec-and-2008105ec-as-regards-priority-substances-in-the431-field-of-water-policy-lex-faoc127344/)
[as-regards-priority-substances-in-the431](https://www.ecolex.org/details/legislation/directive-201339eu-of-the-european-parliament-and430-of-the-council-amending-directives-200060ec-and-2008105ec-as-regards-priority-substances-in-the431-field-of-water-policy-lex-faoc127344/)
[field-of-water-policy-lex-faoc127344/](https://www.ecolex.org/details/legislation/directive-201339eu-of-the-european-parliament-and430-of-the-council-amending-directives-200060ec-and-2008105ec-as-regards-priority-substances-in-the431-field-of-water-policy-lex-faoc127344/).

667 Dewalque, L., Charlier, C., Pirard, C., 2014. Estimated daily intake and cumulative risk
668 assessment of phthalate diesters in a Belgian general population. *Toxicol. Lett.* 231, 161–
669 168. <https://doi.org/10.1016/j.toxlet.2014.06.028>

670

671 Dombret, C., Capela, D., Poissenot, K., Parmentier, C., Bergsten, E., Pionneau, C.,
672 Chardonnet, S., Hardin-Pouzet, H., Grange-Messent, V., Keller, M., Franceschini, I.,
673 Mhaouty-Kodja, S., 2017. Neural Mechanisms Underlying the Disruption of Male Courtship
674 Behavior by Adult Exposure to Di(2-ethylhexyl) Phthalate in Mice. *Environ. Health Perspect.*
675 125, 097001. <https://doi.org/10.1289/EHP1443>

676 EFSA (European Food Safety Authority). 2005. Opinion of the Scientific Panel on food
677 additives, flavourings, processing aids and materials in contact with food (AFC) on a request
678 from the Commission related to bis(2-ethylhexyl)phthalate (DEHP) for use in food contact
679 materials. *EFSA Journal* 3:243; doi: 10.2903/j.efsa.2005.243

680 EFSA (European Food Safety Authority). 2019. Update of the risk assessment of di-
681 butylphthalate (DBP), butyl-benzyl-phthalate (BBP), bis(2-ethylhexyl)phthalate (DEHP), di-
682 isononylphthalate (DINP) and di-isodecylphthalate (DIDP) for use in food contact materials.
683 *EFSA Journal*, 17:5838; doi: 10.2903/j.efsa.2019.5838

684 Erdő, F., Denes, L., de Lange, E., 2017. Age-associated physiological and pathological
685 changes at the blood-brain barrier: A review. *J. Cereb. Blood Flow Metab. Off. J. Int. Soc.*
686 *Cereb. Blood Flow Metab.* 37, 4–24. <https://doi.org/10.1177/0271678X16679420>

687 Gao, D.-W., Wen, Z.-D., 2016. Phthalate esters in the environment: A critical review of their
688 occurrence, biodegradation, and removal during wastewater treatment processes. *Sci. Total*
689 *Environ.* 541, 986–1001. <https://doi.org/10.1016/j.scitotenv.2015.09.148>

690 Hajszan, T., Milner, T.A., Leranthy, C., 2007. Sex Steroids and the Dentate Gyrus. *Prog. Brain*
691 *Res.* 163C, 399–816. [https://doi.org/10.1016/S0079-6123\(07\)63023-4](https://doi.org/10.1016/S0079-6123(07)63023-4)

692 Heneka, M.T., Feinstein, D.L., 2001. Expression and function of inducible nitric oxide
693 synthase in neurons. *J. Neuroimmunol.* 114, 8–18. [https://doi.org/10.1016/s0165-](https://doi.org/10.1016/s0165-5728(01)00246-6)
694 [5728\(01\)00246-6](https://doi.org/10.1016/s0165-5728(01)00246-6)

695 Kabir, E.R., Rahman, M.S., Rahman, I., 2015. A review on endocrine disruptors and their
696 possible impacts on human health. *Environ. Toxicol. Pharmacol.* 40, 241–258.
697 <https://doi.org/10.1016/j.etap.2015.06.009>

698 Kassab, R.B., Lokman, M.S., Essawy, E.A., 2019. Neurochemical alterations following the
699 exposure to di-n-butyl phthalate in rats. *Metab. Brain Dis.* 34, 235–244.
700 <https://doi.org/10.1007/s11011-018-0341-0>

701 Kerr, J.E., Allore, R.J., Beck, S.G., Handa, R.J., 1995. Distribution and hormonal regulation
702 of androgen receptor (AR) and AR messenger ribonucleic acid in the rat hippocampus.
703 *Endocrinology* 136, 3213–3221. <https://doi.org/10.1210/endo.136.8.7628354>

704 Lin, K., Yin, A., Yao, L., Li, Y., 2015. N-myc downstream-regulated gene 2 in the nervous
705 system: from expression pattern to function. *Acta Biochim. Biophys. Sin.* 47, 761–766.
706 <https://doi.org/10.1093/abbs/gmv082>

707 Lu, M.L., Schneider, M.C., Zheng, Y., Zhang, X., Richie, J.P., 2001. Caveolin-1 Interacts with
708 Androgen Receptor A POSITIVE MODULATOR OF ANDROGEN RECEPTOR MEDIATED
709 TRANSACTIVATION. *J. Biol. Chem.* 276, 13442–13451.
710 <https://doi.org/10.1074/jbc.M006598200>

711 Martine, B., Marie-Jeanne, T., Cendrine, D., Fabrice, A., Marc, C., 2013. Assessment of
712 Adult Human Exposure to Phthalate Esters in the Urban Centre of Paris (France). *Bull.*
713 *Environ. Contam. Toxicol.* 90, 91–96. <https://doi.org/10.1007/s00128-012-0859-5>

714 Mhaouty-Kodja, S., 2018. Role of the androgen receptor in the central nervous system. *Mol.*
715 *Cell. Endocrinol.* 465, 103–112. <https://doi.org/10.1016/j.mce.2017.08.001>

716 Obermeier, B., Daneman, R., Ransohoff, R.M., 2013. Development, maintenance and
717 disruption of the blood-brain barrier. *Nat. Med.* 19, 1584–1596.
718 <https://doi.org/10.1038/nm.3407>

719 Picot, M., Billard, J.-M., Dombret, C., Albac, C., Karamah, N., Daumas, S., Hardin-Pouzet,
720 H., Mhaouty-Kodja, S., 2016. Neural Androgen Receptor Deletion Impairs the Temporal
721 Processing of Objects and Hippocampal CA1-Dependent Mechanisms. *PLoS ONE* 11.
722 <https://doi.org/10.1371/journal.pone.0148328>

723 Ran, D., Luo, Y., Gan, Z., Liu, J., Yang, J., 2019. Neural mechanisms underlying the deficit of
724 learning and memory by exposure to Di(2-ethylhexyl) phthalate in rats. *Ecotoxicol. Environ.*
725 *Saf.* 174, 58–65. <https://doi.org/10.1016/j.ecoenv.2019.02.043>

726 Raponi, E., Agenes, F., Delphin, C., Assard, N., Baudier, J., Legraverend, C., Deloulme, J.-
727 C., 2007. S100B expression defines a state in which GFAP-expressing cells lose their neural
728 stem cell potential and acquire a more mature developmental stage. *Glia* 55, 165–177.
729 <https://doi.org/10.1002/glia.20445>

730 Raskin, K., de Gendt, K., Duittoz, A., Liere, P., Verhoeven, G., Tronche, F., Mhaouty-Kodja,
731 S., 2009. Conditional inactivation of androgen receptor gene in the nervous system: effects
732 on male behavioral and neuroendocrine responses. *J. Neurosci. Off. J. Soc. Neurosci.* 29,
733 4461–4470. <https://doi.org/10.1523/JNEUROSCI.0296-09.2009>

734 Robison, L.S., Gannon, O.J., Salinero, A.E., Zuloaga, K.L., 2019. Contributions of sex to
735 cerebrovascular function and pathology. *Brain Res.* 1710, 43–60.
736 <https://doi.org/10.1016/j.brainres.2018.12.030>

737 Saha, R.N., Pahan, K., 2006. Signals for the induction of nitric oxide synthase in astrocytes.
738 *Neurochem. Int.* 49, 154–163. <https://doi.org/10.1016/j.neuint.2006.04.007>

739 Sandoval, K.E., Witt, K.A., 2011. Age and 17 β -estradiol effects on blood-brain barrier tight
740 junction and estrogen receptor proteins in ovariectomized rats. *Microvasc. Res.* 81, 198–205.
741 <https://doi.org/10.1016/j.mvr.2010.12.007>

742 Saunders, N.R., Dziegielewska, K.M., Møllgård, K., Habgood, M.D., 2015. Markers for blood-
743 brain barrier integrity: how appropriate is Evans blue in the twenty-first century and what are
744 the alternatives? *Front. Neurosci.* 9. <https://doi.org/10.3389/fnins.2015.00385>

745 Sierra, A., Navascués, J., Cuadros, M.A., Calvente, R., Martín-Oliva, D., Ferrer-Martín, R.M.,
746 Martín-Estebané, M., Carrasco, M.-C., Marín-Teva, J.L., 2014. Expression of Inducible Nitric
747 Oxide Synthase (iNOS) in Microglia of the Developing Quail Retina. *PLoS ONE* 9.
748 <https://doi.org/10.1371/journal.pone.0106048>

749 Steinwall, O., Klatzo, I., 1966. Selective vulnerability of the blood brain barrier in chemically
750 induced lesions. *J. Neuropath. Exp. Neurol.* 25,: 542-559. [https://doi.org/10.1097/00005072-](https://doi.org/10.1097/00005072-196610000-00004)
751 [196610000-00004](https://doi.org/10.1097/00005072-196610000-00004)

752 Vijitruth, R., Liu, M., Choi, D.-Y., Nguyen, X.V., Hunter, R.L., Bing, G., 2006.
753 Cyclooxygenase-2 mediates microglial activation and secondary dopaminergic cell death in
754 the mouse MPTP model of Parkinson's disease. *J. Neuroinflammation* 3, 6.
755 <https://doi.org/10.1186/1742-2094-3-6>

756 Villaseñor, R., Lampe, J., Schwaninger, M., Collin, L., 2019. Intracellular transport and
757 regulation of transcytosis across the blood–brain barrier. *Cell. Mol. Life Sci.* 76, 1081–1092.
758 <https://doi.org/10.1007/s00018-018-2982-x>

759 Vodo, S., Bechi, N., Petroni, A., Muscoli, C., Aloisi, A.M., 2013. Testosterone-Induced Effects
760 on Lipids and Inflammation [WWW Document]. *Mediators Inflamm.*
761 <https://doi.org/10.1155/2013/183041>

762 Weiss, N., Miller, F., Cazaubon, S., Couraud, P.-O., 2009. The blood-brain barrier in brain
763 homeostasis and neurological diseases. *Biochim. Biophys. Acta BBA - Biomembr.*, Apical
764 Junctional Complexes Part II 1788, 842–857. <https://doi.org/10.1016/j.bbamem.2008.10.022>

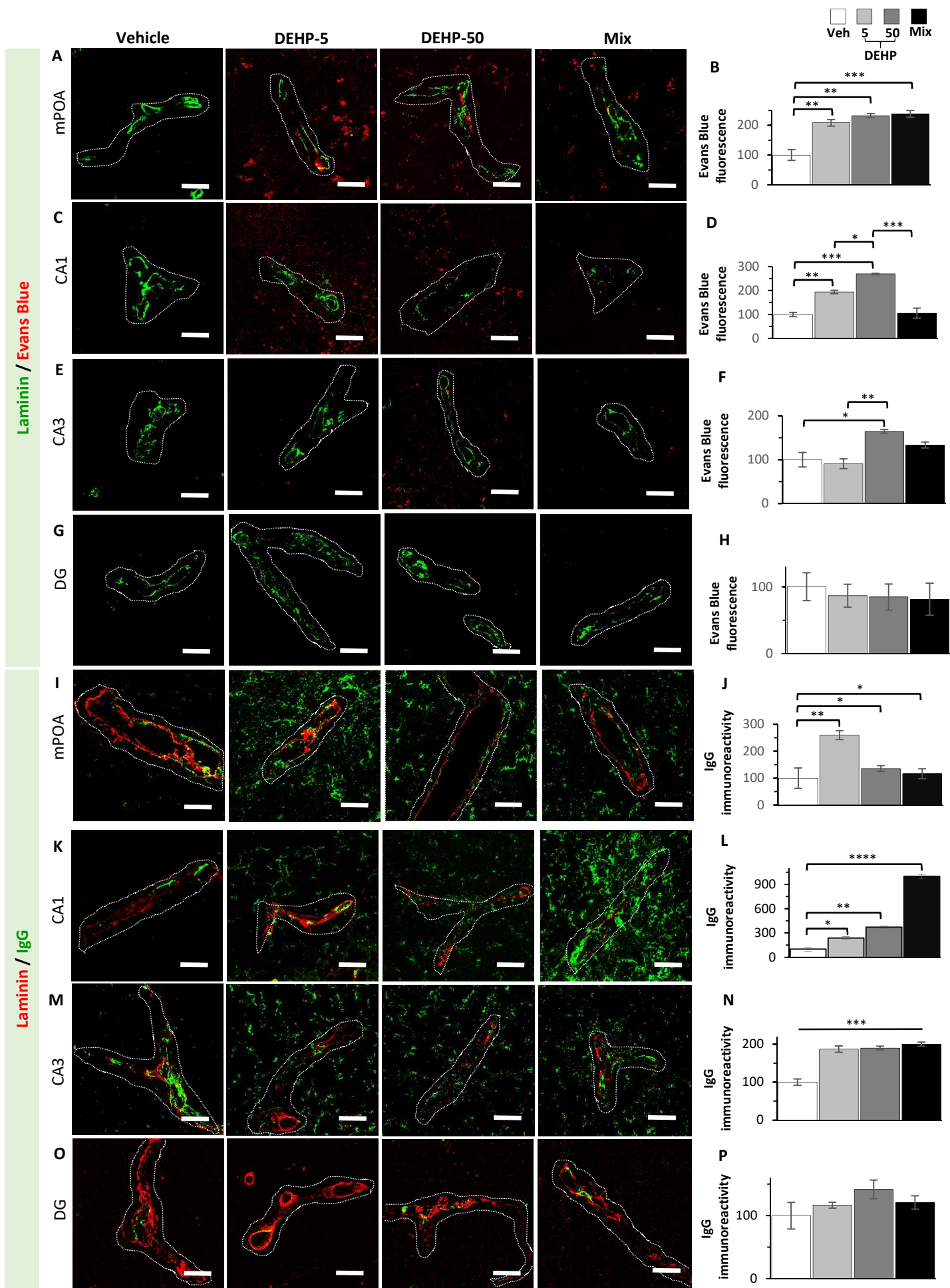
765 Werner, C., Reeker, W., Engelhard, K., Lu, H., Kochs, E., 1997. [Ketamine racemate and S-
766 (+)-ketamine. Cerebrovascular effects and neuroprotection following focal ischemia].
767 *Anaesthesist* 46 Suppl 1, S55-60

768 Xu, X., Yang, Y., Wang, R., Wang, Y., Ruan, Q., Lu, Y., 2015. Perinatal exposure to di-(2-
769 ethylhexyl) phthalate affects anxiety- and depression-like behaviors in mice. *Chemosphere*
770 124, 22–31. <https://doi.org/10.1016/j.chemosphere.2014.10.056>

771 You, M., Dong, J., Fu, Y., Cong, Z., Fu, H., Wei, L., Wang, Yi, Wang, Yuan, Chen, J., 2018.
772 Exposure to Di-(2-ethylhexyl) Phthalate During Perinatal Period Gender-Specifically Impairs
773 the Dendritic Growth of Pyramidal Neurons in Rat Offspring. *Front. Neurosci.* 12.
774 <https://doi.org/10.3389/fnins.2018.00444>

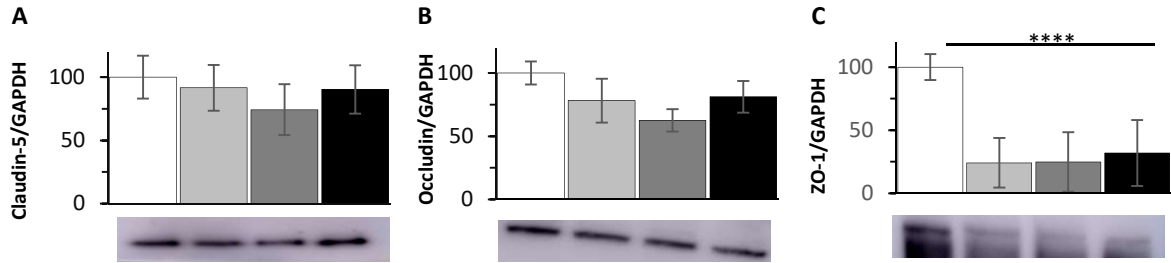
775

776

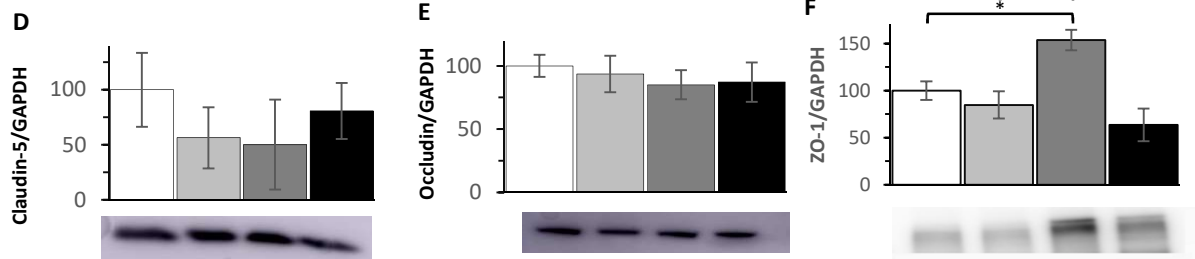


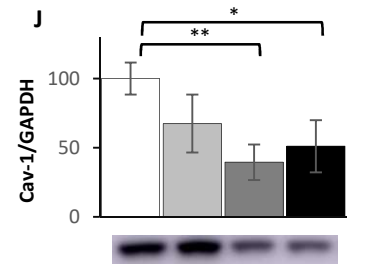
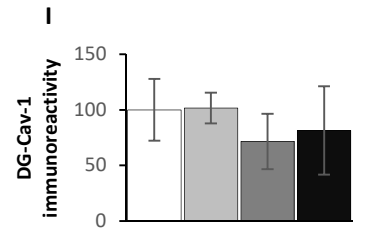
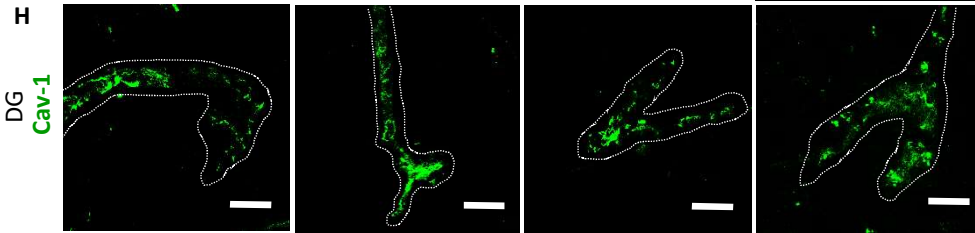
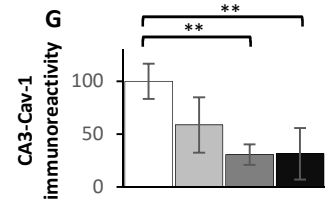
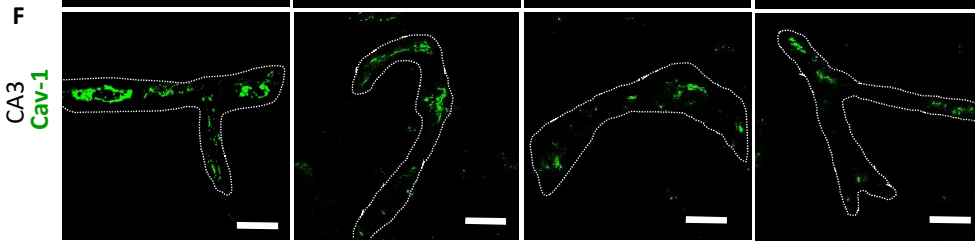
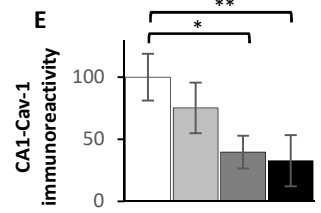
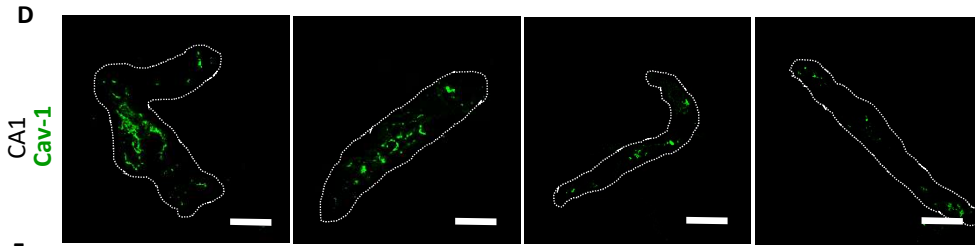
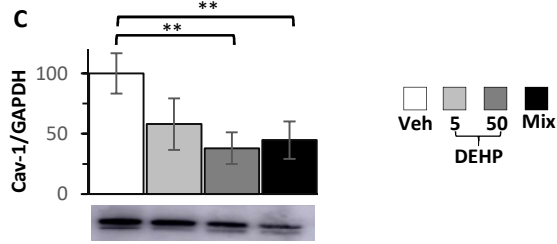
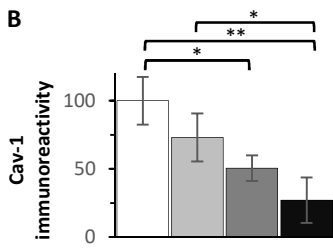
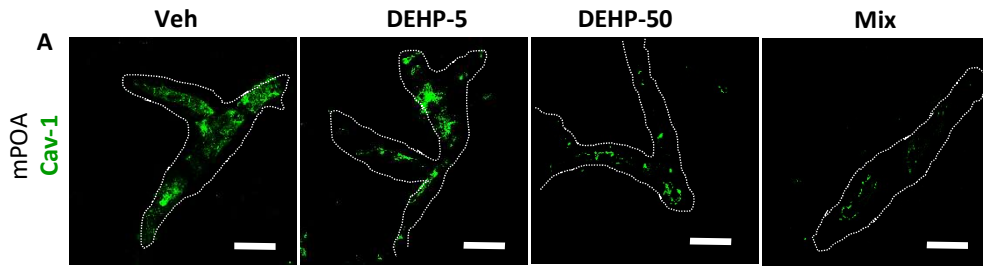
mPOA

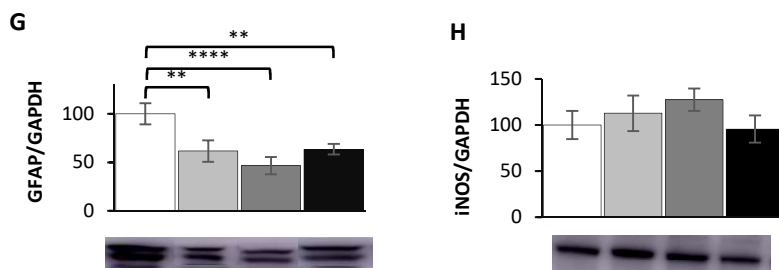
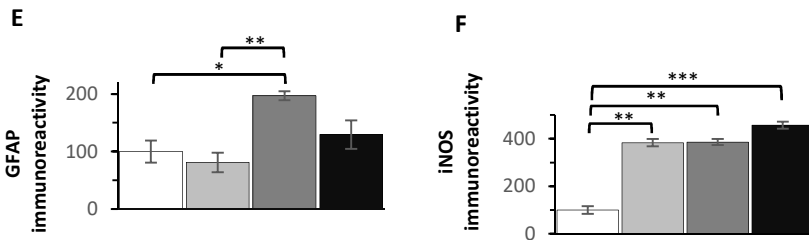
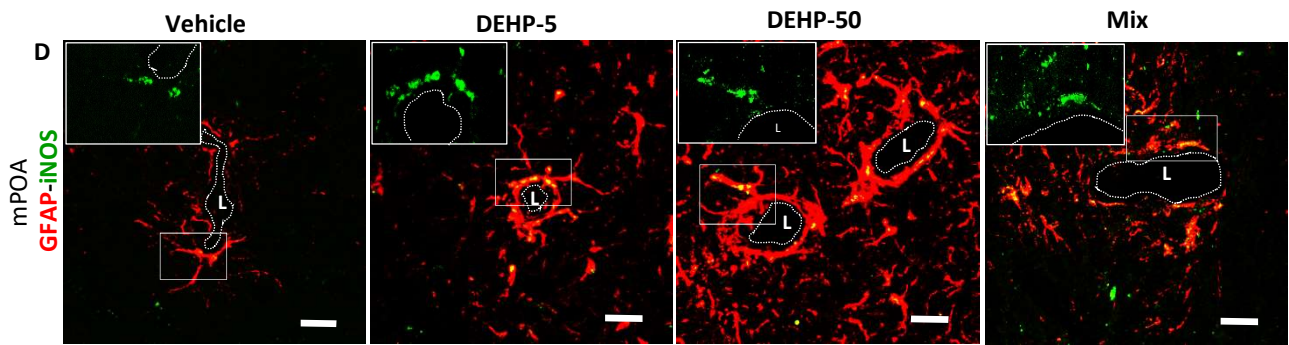
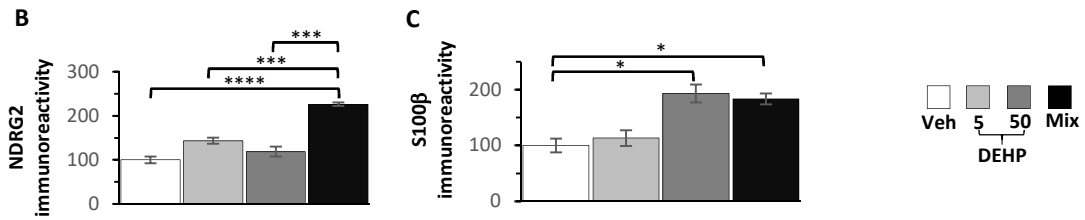
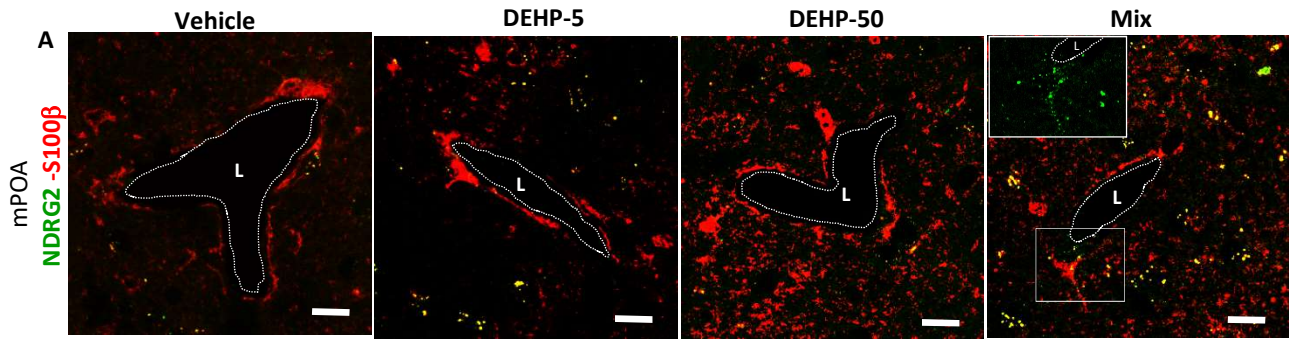
Veh 5 50 Mix
DEHP

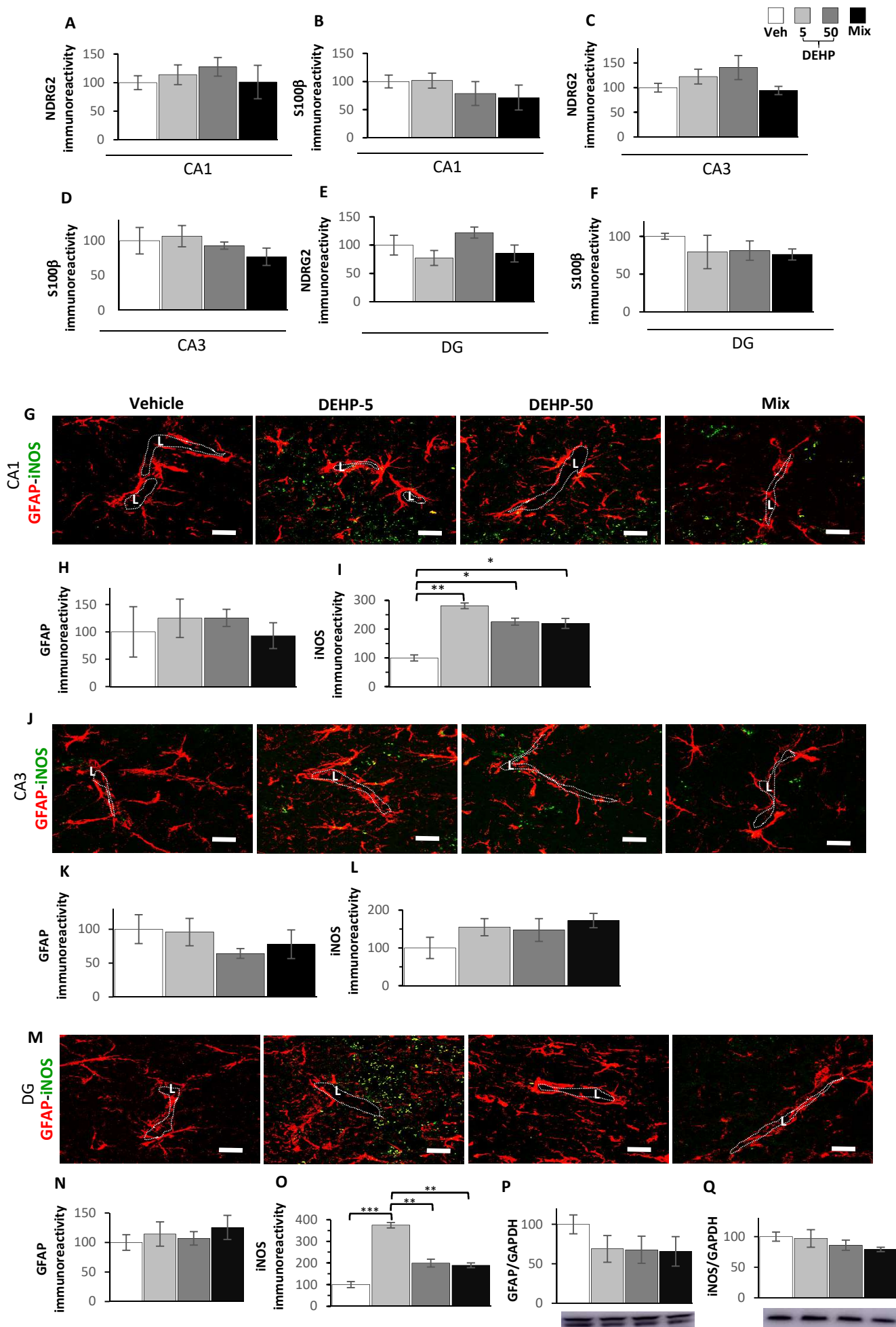


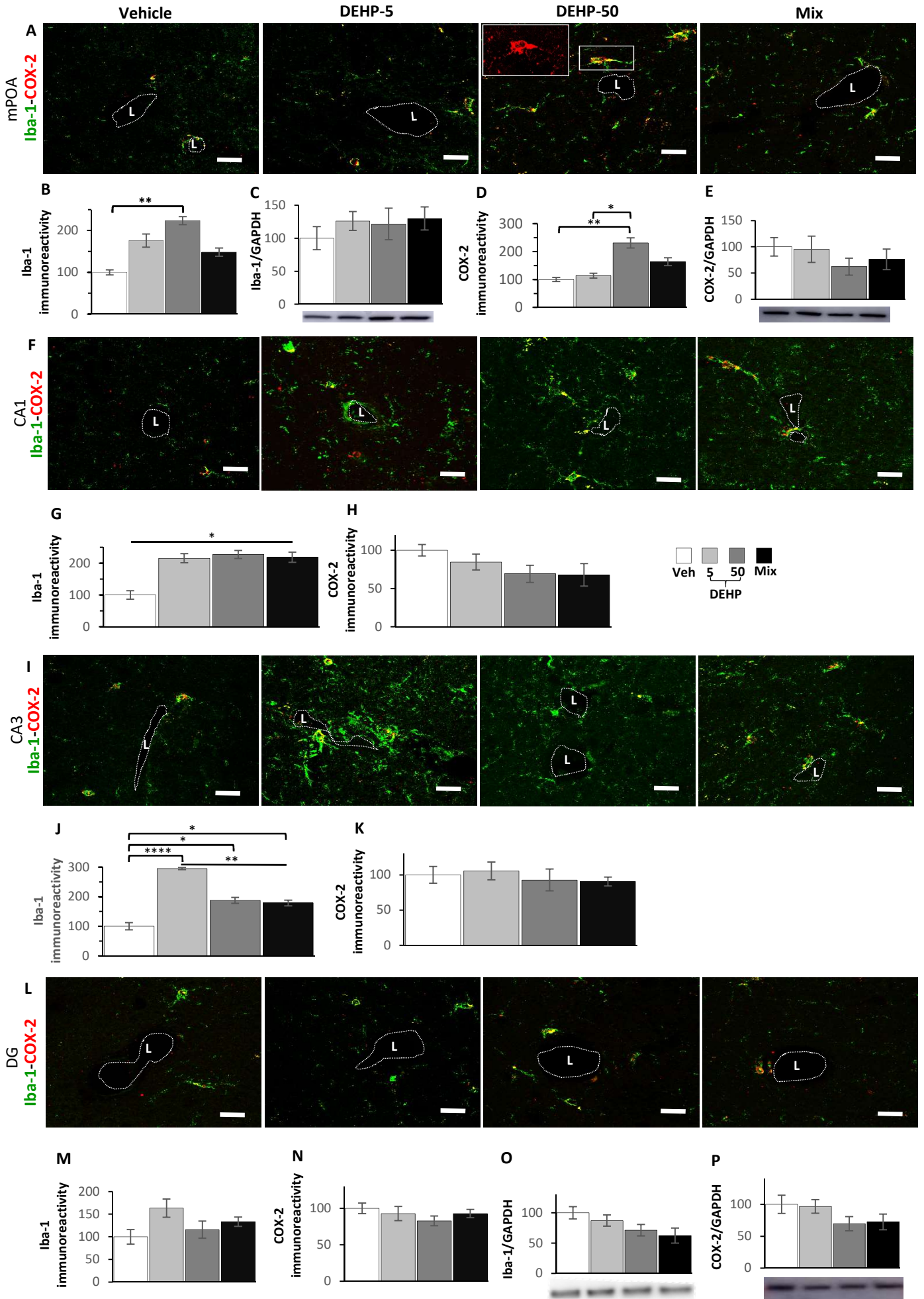
Hippocampus











1 **Figure legends**

2 **Figure 1. Exposure to DEHP alone or in a phthalate mixture increased BBB permeability** 3 **to Evans blue dye and endogenous IgG.**

4 The permeability of BBB was analyzed using Evans blue dye (n=3 per group, A to H) and
5 immunolabeled endogenous IgG (n=5 per group, I to P) in the hypothalamic medial preoptic
6 area (mPOA) and hippocampal CA1, CA3 and DG. Images were selected from brain sections
7 containing the sub-regions of interest in adult male mice orally exposed to vehicle (Veh; first
8 column), DEHP at 5 µg/kg/d (DEHP-5; second column), DEHP at 50 µg/kg/d (DEHP-50; third
9 column) and a phthalate mixture (Mix; fourth column). (A-H) Representative images and
10 corresponding quantitative analysis of the six to eight serial sections for each brain examined
11 of the mPOA (A, B), CA1 (C, D), CA3 (E, F) and DG (G, H) for Evans blue dye tracer (red),
12 capillaries were labeled with anti-laminin (green). (I-P) Representative images and
13 corresponding quantitative analysis of the six to eight serial sections for each brain examined
14 of the mPOA (I, J), CA1 (K, L), CA3 (M, N) and DG (O, P) of endogenous circulating IgG
15 (green), capillaries were labeled with anti-laminin (red).

16 * $p < 0.05$; ** $p < 0.01$; *** $p < 0.001$; **** $p < 0.0001$ compared to vehicle-treated mice compared
17 to the vehicle group. All data are expressed as mean percentages \pm S.E.M of vehicle (100%).

18 The pictures presented are the projection of 3 successive optical sections (1 µm) into one
19 image.

20 Scale bar: 10 µm. The dotted lines delimit the outer contour of the capillaries. The
21 quantifications of fluorescence density were measured over the entire surface of the images.

22

23 **Figure 2. Exposure to DEHP alone or in a phthalate mixture affected endothelial tight** 24 **junction protein ZO-1 levels but not claudin-5 and occludin protein levels.**

25 Western blot analysis (n = 6 per treatment group) of tight junction proteins performed on
26 microvessel-enriched fractions from hypothalamus (A-C) and hippocampus (D-F) of mice
27 exposed to the Vehicle (Veh), DEHP at 5 µg/kg/d (DEHP-5), DEHP at 50 µg/kg/d (DEHP-50)
28 or the phthalate mixture (Mix). All data are expressed as mean percentages ± S.E.M of vehicle
29 (100%). **p* < 0.05; ***p* < 0.01; ****p* < 0.001; *****p* < 0.0001 compared to the vehicle group. Data
30 were normalized to GAPDH level.

31

32 **Figure 3. Exposure to DEHP alone or in a phthalate mixture decreased protein levels of**
33 **the caveolae-associated membrane protein Cav-1.**

34 Images were selected from brain sections containing the sub-regions of interest in adult male
35 mice orally exposed to vehicle (Veh; first column), DEHP at 5 µg/kg/d (DEHP-5; second
36 column), DEHP at 50 µg/kg/d (DEHP-50; third column) and a phthalates mixture (Mix; fourth
37 column). (A, B) Representative images of immunodetection of Cav-1 in the mPOA (A) and the
38 corresponding quantitative analysis of the Cav-1 immunoreactivity density (B) of the six to eight
39 serial sections for each brain examined (n = 5 per treatment group). Values represent mean
40 percentages ± S.E.M of vehicle (100%). **p* < 0.05; ***p* < 0.01 compared to the vehicle group.
41 (C) Western blot analysis of Cav-1 performed on microvessel-enriched fractions. **p* < 0.05; ***p*
42 < 0.01 compared to the vehicle group (n = 6 per treatment group). Data were normalized to
43 GAPDH levels.

44 (D-I) Representative images of immunodetection of Cav-1 in the hippocampus (D: CA1; F:
45 CA3; H: DG) and the corresponding quantitative analysis of the Cav-1 immunoreactivity
46 density (E: CA1; G: CA3; I: DG) of the six to eight serial sections for each brain examined (n=5
47 per group). **p* < 0.05; ***p* < 0.01 compared to the vehicle group. (J) Western blot analysis of
48 Cav-1 performed on microvessel-enriched fractions from hippocampus. **p* < 0.05; ***p* < 0.01
49 compared to the vehicle group (n = 6 per treatment group). Data were normalized to GAPDH
50 level.

51 Scale bar: 10 μ m. The dotted lines delimit the outer contour of the capillaries. The
52 quantifications of fluorescence density were measured over the entire surface of the images.
53 All values represent mean percentages \pm S.E.M of vehicle (100%).

54

55 **Figure 4. Exposure to DEHP alone or in a phthalate mixture induced astrocyte activation**
56 **and iNOS expression in the medial preoptic area (mPOA).**

57 (A-C) Representative images (A) and corresponding quantitative analysis (B, C) of the six to
58 eight serial sections for each brain examined of the co-immunolabeling of NDRG2 (green,
59 insert) and S100 β (red) in the mPOA of mice exposed to the vehicle (Veh), DEHP at 5 μ g/kg/d
60 (DEHP-5), DEHP at 50 μ g/kg/d, or phthalate mixture (Mix) (n = 5 per treatment group). (D-F)
61 Representative images (D) and corresponding quantitative analysis (E, F) of the six to eight
62 serial sections for each brain examined of the co-immunolabeling of iNOS (green, inserts) and
63 GFAP (red) in the mPOA (n=5 per group). * p < 0.05; *** p < 0.001; **** p < 0.0001 compared to
64 the vehicle group.

65 (G, H) Western blot analysis (n = 6 per treatment group) of GFAP (G) and iNOS (H) performed
66 on microvessel-enriched fractions from the hypothalamus. * p < 0.05; ** p < 0.01; *** p < 0.001;
67 **** p < 0.0001 compared to the vehicle group (n=6 per group). Data were normalized to
68 GAPDH level.

69 Scale bar: 10 μ m. L: Lumen delimited by the dotted lines. The quantifications of fluorescence
70 density were measured over the entire surface of the images. All values represent mean
71 percentages \pm S.E.M of vehicle (100%).

72

73 **Figure 5. Exposure to DEHP alone or in a phthalate mixture had no effect on astrocyte**
74 **activation in the hippocampus but induced iNOS expression in the CA1 and DG.**

75 (A-F) Quantitative analysis of the immunoreactivity of NDRG2 and S100 β in the hippocampus
76 (A, B: CA1; C D: CA3; E, F: DG) of the six to eight serial sections for brain collected from mice
77 exposed to the vehicle (Veh), DEHP at 5 μ g/kg/d (DEHP-5), DEHP at 50 μ g/kg/d, or phthalate
78 mixture (Mix) (n = 5 per treatment group). No significant difference was measured compared
79 to vehicle-treated controls.

80 (G-O) Representative images of co-immunodetection of GFAP (red) and iNOS (green) in the
81 hippocampus (G: CA1; J: CA3; M: DG) and their corresponding quantitative analysis of the
82 immunoreactivity density (H, I: CA1; K, L: CA3; N, O: DG) of the six to eight serial sections for
83 each brain examined (n=5 per group). * p < 0.05; ** p < 0.01; *** p < 0.001 compared to vehicle-
84 treated controls.

85 (P, Q) Western blot analysis (n=6 per group) of GFAP (P) and iNOS (Q) performed on
86 microvessel-enriched fractions from hippocampus. Data were normalized to GAPDH level. No
87 significant difference was measured compared to vehicle-treated controls.

88 Scale bar: 10 μ m. L: Lumen delimited by the dotted lines. The quantifications of fluorescence
89 density were measured over the entire surface of the images. All values represent mean
90 percentages \pm S.E.M of vehicle (100%).

91

92 **Figure 6. Exposure to DEHP alone or in a phthalate mixture induced microglia activation**
93 **in the testosterone-sensitive cerebral regions, the medial preoptic area (mPOA) and the**
94 **hippocampus, and increased COX-2 expression in the mPOA.**

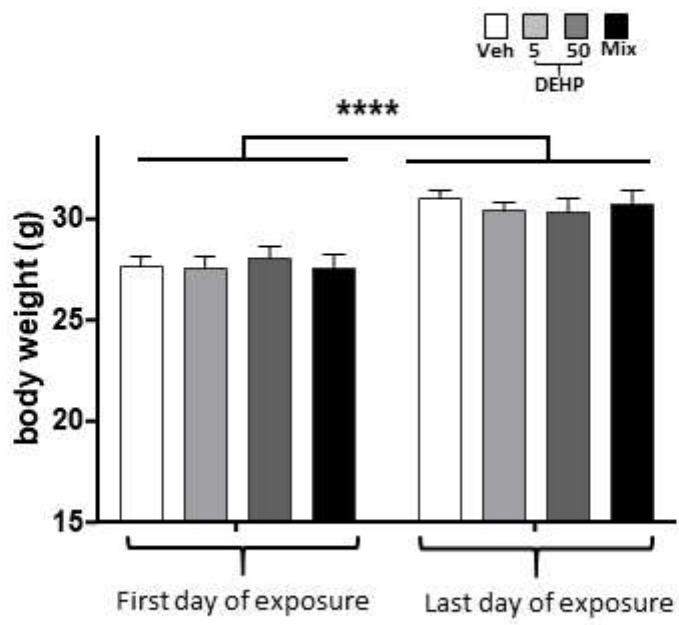
95 (A, B, D) Representative images (A) and corresponding quantitative analysis (B, D) of the six
96 to eight serial sections for each brain examined of the co-immunolabeling of Iba-1 (green) and
97 COX-2 (red, insert) in the mPOA of mice exposed to the vehicle (Veh), DEHP at 5 μ g/kg/d
98 (DEHP-5), DEHP at 50 μ g/kg/d, or phthalate mixture (Mix) (n = 5 per treatment group). * p <
99 0.05; ** p < 0.01 compared to the vehicle group. (C, E) Western blot analysis (n = 6 per
100 treatment group) of Iba-1 (C) and COX-2 (E) performed on microvessel-enriched fractions from

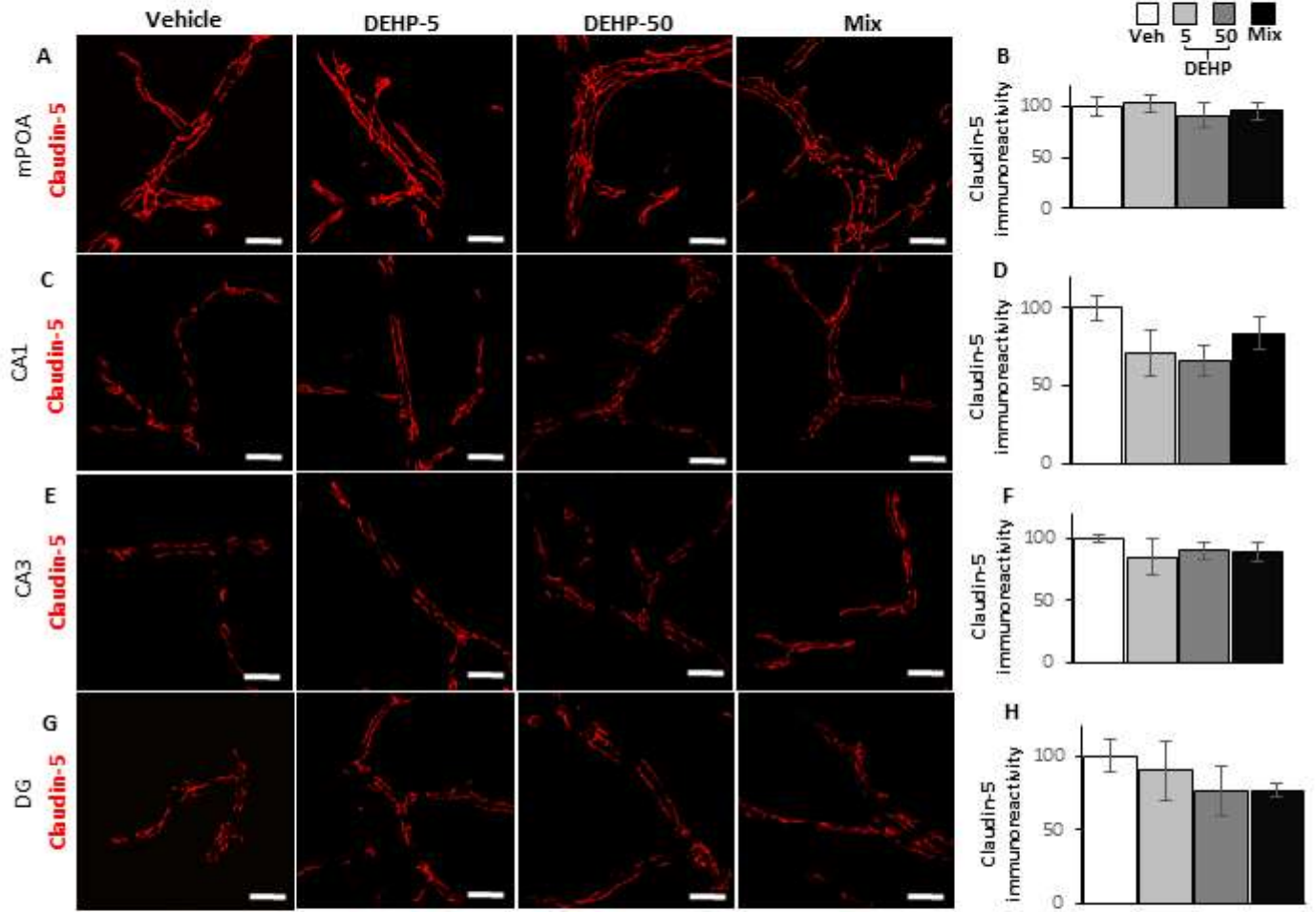
101 hypothalamus. * $p < 0.05$; ** $p < 0.01$ compared to the vehicle group. Data were normalized to
102 GAPDH level.

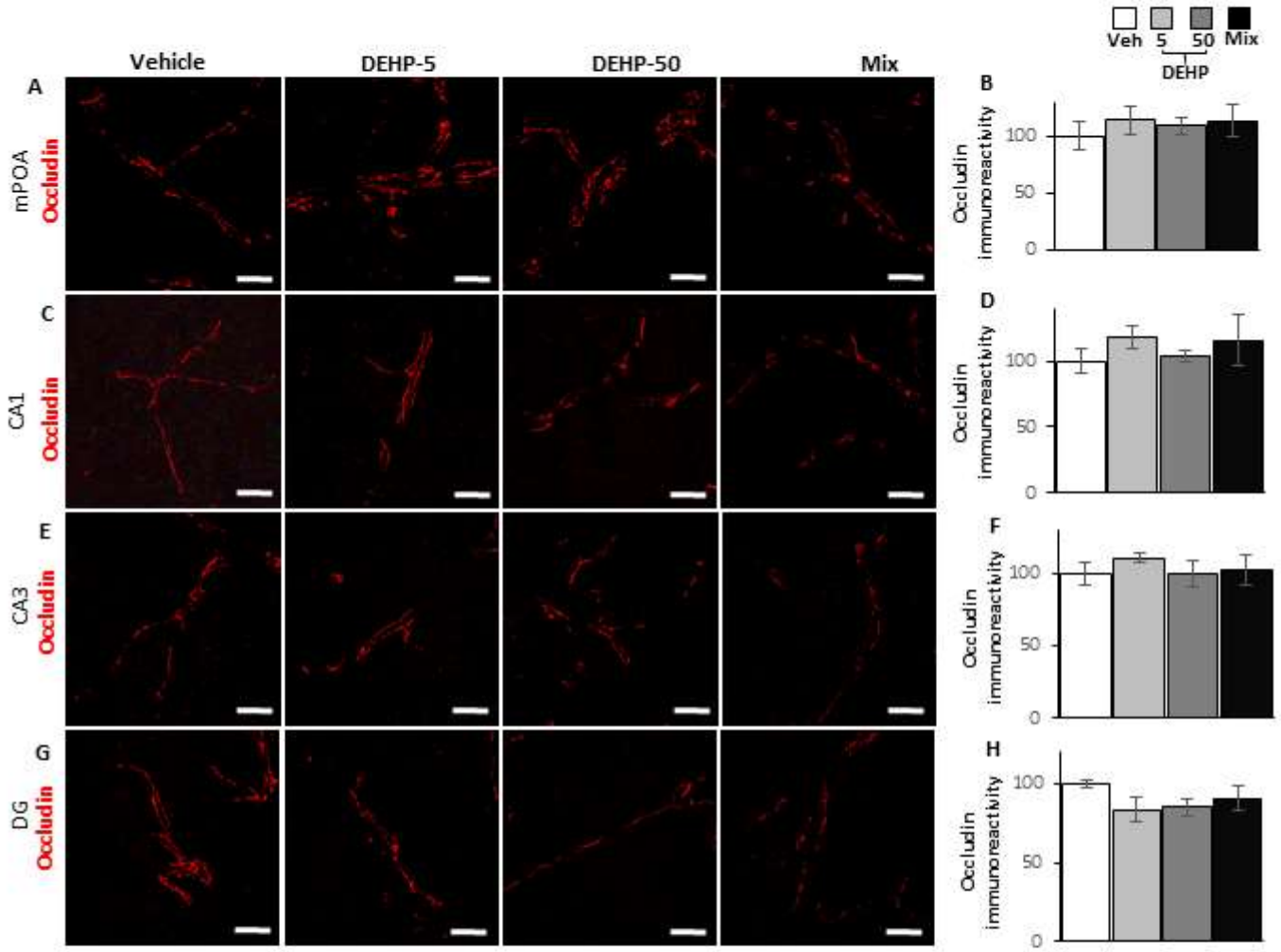
103 (F-N) Representative images of co-immunodetection of Iba-1 (green) and COX-2 (red) in the
104 hippocampus (F: CA1; I: CA3; L: DG) and their corresponding quantitative analysis of the
105 immunoreactivity density (G, H: CA1; J, K: CA3; M, N: DG) of the six to eight serial sections
106 for each brain examined ($n = 5$ per treatment group). * $p < 0.05$; ** $p < 0.01$; *** $p < 0.001$; **** p
107 < 0.0001 compared to vehicle-treated controls. (O, P) Western blot analysis ($n = 6$ per
108 treatment group) of Iba-1 (O) and COX-2 (P) performed on microvessel-enriched fractions from
109 hippocampus. Data were normalized to GAPDH level. No significant difference was measured
110 compared to vehicle-treated controls.

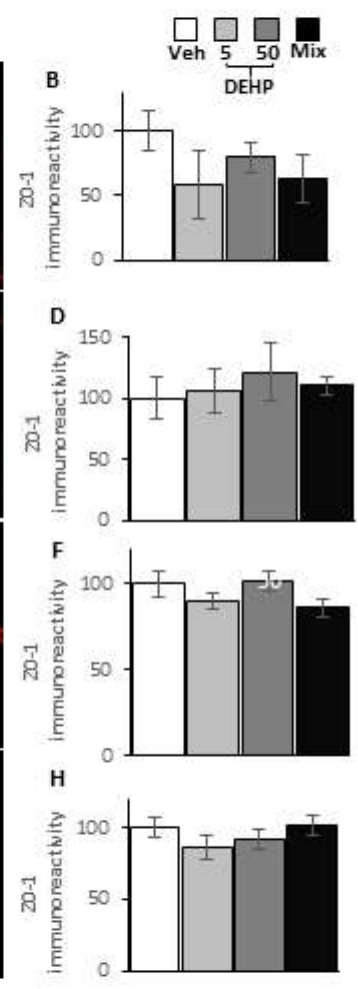
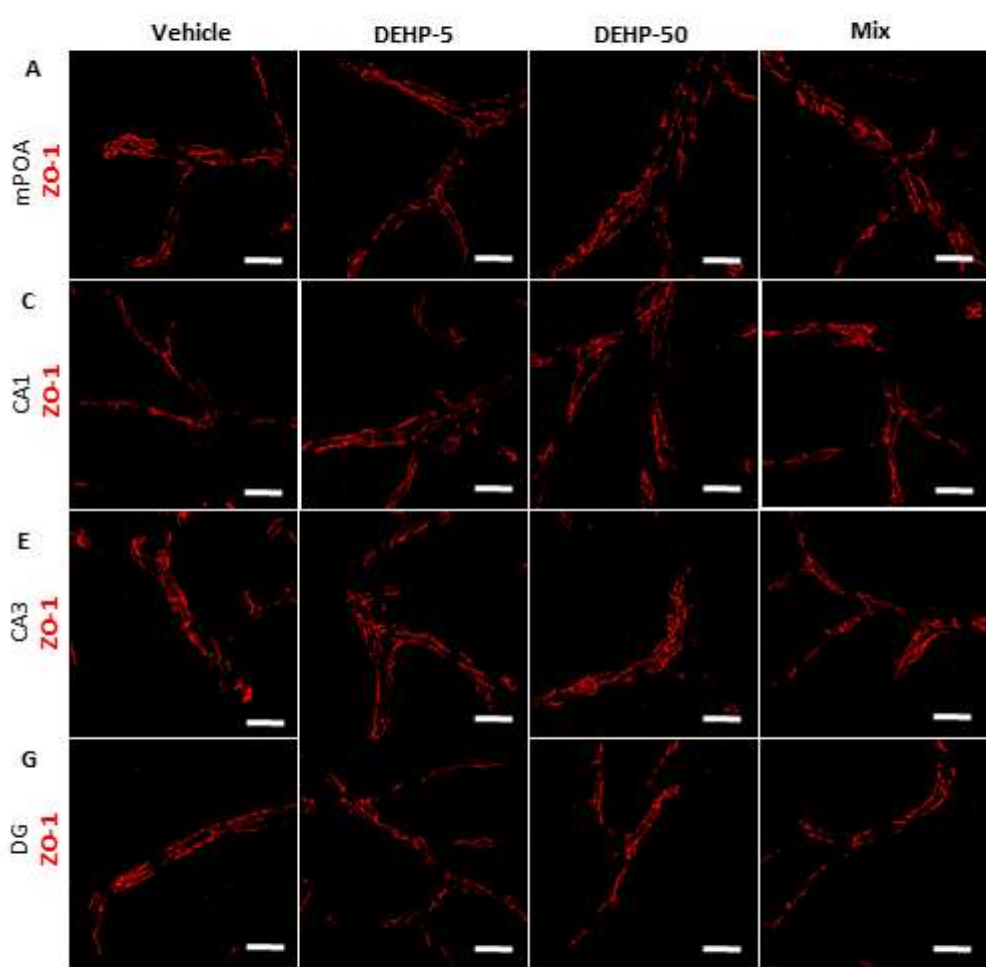
111 Scale bar: 10 μm . L: Lumen delimited by the dotted lines. The quantifications of fluorescence
112 density were measured over the entire surface of the images. All values represent mean
113 percentages \pm S.E.M of the vehicle (100%).

114









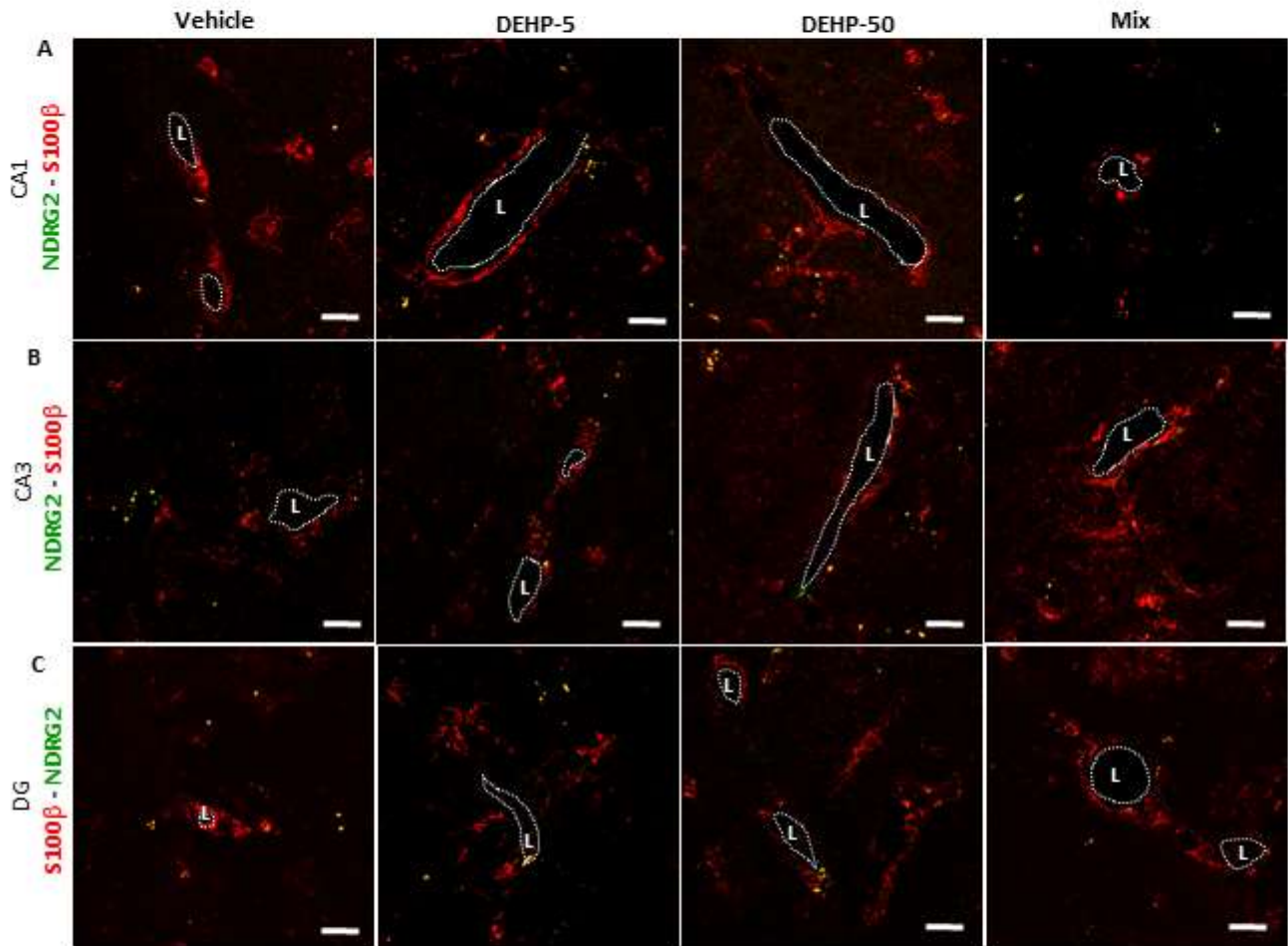


Figure S1. Exposure to DEHP alone or in a phthalate mixture did not affect the body weight of treated mice.

The body weight of male mice exposed to the vehicle (Veh), DEHP at 5 µg/kg/d (DEHP-5), DEHP at 50 µg/kg/d (DEHP-50), or a phthalate mixture (Mix), is reported for the first and last days of exposure. The values represent body weight means (g) ± S.E.M (n = 12 per treatment group). There was an effect of time ($F_{(1, 88)} = 48.8$, $p < 0,0001$) but not of treatment ($F_{(3, 88)} = 0,1063$, $p = 0.9562$).

Figure S2. Exposure to DEHP alone or in a phthalate mixture did not affect claudin-5 immunoreactivity.

(A, B) Representative images of immunodetection of claudin-5 in the mPOA of mice exposed to the vehicle (Veh), DEHP at 5 µg/kg/d (DEHP-5), DEHP at 50 µg/kg/d (DEHP-50), or phthalate mixture (Mix) (A) and their corresponding quantitative analysis of the immunoreactivity density (B) of the six to eight serial sections for each brain examined (n = 5 per treatment group). No significant difference was measured compared to vehicle-treated controls. (C-H) Representative images of immunodetection of claudin-5 (C: CA1; E: CA3; G: DG) and the corresponding quantitative analysis of the immunoreactivity density (D: CA1; F: CA3; H: DG) of the six to eight serial sections for each brain examined (n=5 per group). No significant difference was measured compared to vehicle-treated controls.

Scale bar: 10 µm. The quantifications of fluorescence density were measured over the entire surface of the images and the values represent mean percentages ± S.E.M of vehicle (100%).

Figure S3. Exposure to DEHP alone or in a phthalate mixture did not affect occludin immunoreactivity.

(A, B) Representative images of immunodetection of occludin in the mPOA of mice exposed to the vehicle (Veh), DEHP at 5 $\mu\text{g}/\text{kg}/\text{d}$ (DEHP-5), DEHP at 50 $\mu\text{g}/\text{kg}/\text{d}$ (DEHP-50), or phthalate mixture (Mix) (A) and their corresponding quantitative analysis of the immunoreactivity density (B) of the six to eight serial sections for each brain examined (n=5 per group). No significant difference was measured compared to vehicle-treated controls. (C-H) Representative images of immunodetection of occludin in the hippocampus (C: CA1; E: CA3; G: DG) and the corresponding quantitative analysis of the immunoreactivity density (D: CA1; F: CA3; H: DG) of the six to eight serial sections for each brain examined (n = 5 per treatment group). No significant difference was measured compared to vehicle-treated controls.

Scale bar: 10 μm . The quantifications of fluorescence density were measured over the entire surface of the images and the values represent mean percentages \pm S.E.M of vehicle (100%).

Figure S4. Exposure to DEHP alone or in a phthalate mixture did not affect ZO-1 immunoreactivity.

(A, B) Representative images of immunodetection of ZO-1 in the mPOA of mice exposed to the vehicle (Veh), DEHP at 5 $\mu\text{g}/\text{kg}/\text{d}$ (DEHP-5), DEHP at 50 $\mu\text{g}/\text{kg}/\text{d}$ (DEHP-50), or a phthalate mixture (Mix) (A) and their corresponding quantitative analysis of the immunoreactivity density (B) of the six to eight serial sections for each brain examined (n=5 per group). No significant difference was measured compared to vehicle-treated controls. (C-H) Representative images of immunodetection of ZO-1 in the hippocampus (C: CA1; E: CA3; G: DG) and the corresponding quantitative analysis of the immunoreactivity density (D: CA1; F: CA3; H: DG) of the six to eight

serial sections for each brain examined (n = 5 per treatment group). No significant difference was measured compared to vehicle-treated controls.

Scale bar: 10 μm . The quantifications of fluorescence density were measured over the entire surface of the images and the values represent mean percentages \pm S.E.M of vehicle (100%).

Figure S5. Exposure to DEHP alone or in a phthalate mixture did not affect NDRG2 and S100 β immunoreactivity in the hippocampus.

Representative images of co-immunodetection of NDRG2 (green) and S100 β (red) in the hippocampal CA1 (A), CA3 (B) and DG (C) of mice exposed to the vehicle (Veh), DEHP at 5 $\mu\text{g}/\text{kg}/\text{d}$ (DEHP-5), DEHP at 50 $\mu\text{g}/\text{kg}/\text{d}$ (DEHP-50), or phthalate mixture (Mix).

Scale bar: 10 μm . L: Lumen delimited by the dotted lines.

Table 1: List of primary antibodies

Antibody	Host	Manufacturer	Catalog no	Application	Working dilution
NDRG2	Rabbit	Cell Signaling Technology	5667S	IHC	1/400
S100 β	Mouse	Sigma-Aldrich	s2532	IHC	1/1000
COX-2	Goat	Santa Cruz	Sc-1747	IHC - WB	1/200
Iba-1	Rabbit	WAKO	016-20001	WB	1/500
Iba-1	Rabbit	Biocare Medical	CP-290	IHC	1/300
ZO-1	Rabbit	Invitrogen	61-7300	IHC - WB	1/125 - 1/500
Claudin-5	Rabbit	Invitrogen	34-1600	IHC - WB	1/500
Cav-1	Mouse	Biosciences	610407	IHC	1/200
Cav-1	Mouse	Santa Cruz	sc-53564	WB	1/200
iNOS	Mouse	Santa Cruz	sc-7271	WB	1/200
iNOS	Mouse	Sigma-Aldrich	n9657	IHC	1/1000
GFAP	Mouse	Sigma-Aldrich	G3893	WB	1/500
GFAP	Rabbit	DAKO	Z0334	IHC	1/500
Laminin	Rabbit	Sigma-Aldrich	L9393	IHC - WB	1/200 - 1/100
Occludin	Rabbit	Invitrogen	40-4700	IHC - WB	1/500 - 1/250
GAPDH	Mouse	Santa Cruz	sc-32233	WB	1/10000

IHC: Immunohistochemistry; WB: Western blotting

Table 2: Synthesis of the effects of an oral exposure during adulthood to low doses of DEHP alone or in phthalate mixture in male mice on BBB integrity and associated inflammation in the hypothalamus and hippocampus

		Immunohistochemistry analysis				Western blot analysis	
		mPOA	CA1	CA3	DG	Hypothalamus	Hippocampus
BBB integrity	Permeability						
	<i>Evans blue extravasation</i>	increased: DEHP-5, DEHP-50 and Mix	increased: DEHP-5 and DEHP-50	increased: DEHP-50	not affected	n.d.	n.d.
	<i>Endogenous IgG extravasation</i>	increased: DEHP-5, DEHP-50 and Mix	increased: DEHP-5, DEHP-50 and Mix	increased: DEHP-5, DEHP-50 and Mix	not affected	n.d.	n.d.
	Endothelial tight junctions						
	<i>Claudin-5</i>	not affected	not affected	not affected	not affected	not affected	not affected
	<i>Occludin</i>	not affected	not affected	not affected	not affected	not affected	not affected
	<i>ZO-1</i>	not affected	not affected	not affected	not affected	decreased: DEHP-5, DEHP-50 and Mix	increased: DEHP-50
	Trans-endothelial vesicular transport						
	<i>Cav-1</i>	decreased: DEHP-50 and Mix	decreased: DEHP-50 and Mix	decreased: DEHP-50 and Mix	not affected	decreased: DEHP-50 and Mix	decreased: DEHP-50 and Mix
Inflammation							
	Astrocyte activation						
	<i>NDRG2</i>	increased: Mix	not affected	not affected	not affected	n.d.	n.d.
	<i>S100 β</i>	increased: DEHP-50 and Mix	not affected	not affected	not affected	n.d.	n.d.
	<i>GFAP</i>	increased: DEHP-50	not affected	not affected	not affected	decreased: DEHP-5, DEHP-50 and Mix	not affected
	Microglia activation						
	<i>Iba-1</i>	increased: DEHP-50	increased: DEHP-5, DEHP-50 and Mix	increased: DEHP-5, DEHP-50 and Mix	not affected	not affected	not affected
	Inflammatory molecules						
	<i>iNOS</i>	increased: DEHP-5, DEHP-50 and Mix	increased: DEHP-5, DEHP-50 and Mix	not affected	increased: DEHP-5	not affected	not affected
	<i>COX-2</i>	increased: DEHP-50	not affected	not affected	not affected	not affected	not affected

n.d.: not determined; DEHP-5: DEHP at 5µg/kg/d; DEHP-50: DEHP at 50 µg/kg/d; Mix: phthalate mixture